Author Response to Reviewer Comments

Dear Editor and Reviewers,

We would like to thank the reviewers for the time they put into reading and commenting on the manuscript. Their remarks and constructive criticism surely helped to improve the quality of this paper. Below you will find our responses to the referee comments, starting with our response to reviewer #1 and followed by our response to reviewer #2 (Stefan Hendricks). The changes made to the manuscript can be found at the end of this document.

Steven Fons and Nathan Kurtz

Reviewer 1:

Summary: This paper investigates whether the considerable scattering of satellite radar altimetry at Ku-Band, namely CryoSat-2, that can be expected to occur at the air-snow interface can be exploited to estimate the elevation of the air-snow interface relative to the ocean surface and hence get an estimate of the total (sea ice + snow) freeboard. To do so a two-layer physical model is used together with least square fitting to obtain a fitted waveform to CryoSat-2 Level 1B data from which the elevations are obtained for lat winter / spring October months of 2011-2017. CryoSat-2 elevations are compared with observations from Operation Ice Bridge airborne topographic mapper for two quasi-coincident OIB-CS-2 overflights, one in 2011, one in 2012. Total freeboard is computed and averaged over the entire period 2011-2017 for the entire Antarctic and discussed and compared with ICESat total freeboard maps. Also, the potential to combine air-snow and ice-snow interface elevations for snow depth on sea ice retrieval is tested. While first evaluation results are promising and suggest that total freeboard derived from CS-2 could potentially be used complementary to ICESat and ICESat-2 data more work is required to better understand the observed differences between CS-2 total freeboard and independent data.

I find this an interesting and important contribution to the existing literature and suggest publication of the research results - provided that the authors take into account the various, partly substantial, suggestions for a major revision of their manuscript. I list my major concerns below in the general comments.

We sincerely thank the reviewer for his/her thoughtful and detailed comments on the manuscript. Particularly, we appreciate the suggestions on ways to strengthen the CryoSat-2/Operation IceBridge comparison as well as the encouragement to include more and (more applicable) references to recent studies on Antarctic sea ice freeboard retrievals. Our responses (in blue) to the reviewer comments (in black) can be found below.

General comments: GC1: The introduction lacks to present the state-of-the-art of seaice and/or total freeboard retrieval in the Antarctic. Several studies exist that are using radar or laser altimeter data for this kind of retrieval. In addition, the introduction lacks to present the state-of-the-art of freeboard-to-thickness conversion and inherent problems and uncertainties. While mitigation of the former lack is required to understand why it might make sense to try to derive total freeboard also from CS-2 data, mitigation of the latter lack is required to understand your attempt to retrieve snow depth on sea ice as well.

The introduction was indeed lacking in the original version of the manuscript. It has been substantially revised to focus on Antarctic retrievals of sea ice freeboard, referencing methods from laser altimetry (Zwally et al., 2008; Kurtz and Markus, 2012; Kern et al., 2016; Li et al., 2018) as well as radar altimetry (Giles et al., 2008; Schwegmann et al., 2016; Paul et al., 2018). Additionally, information on present day freeboard to thickness conversions is included as motivation for retrieving snow depth. We address the current snow depths used in thickness calculations, which range from passive microwave data, to assumptions that snow depth = total freeboard, to parameterizations of the snow depth based on multi-year ice fraction and total freeboard. The revised introduction can be found in section 1 of the revised manuscript.

GC2: I don't find the interpretation of Figures 3 and 4 particularly convincing as a motivation why there is substantial(ly more) information about the air-snow interface in the echograms of the snow radar and the Ku-Band altimeter. See my respective specific comments.

These figures are meant to show that Ku-band returns of the air-snow interface are similar to air-snow interface returns from the snow radar. Since the snow radar is utilized often for snow depth retrievals, similar returns from the Ku-band would provide evidence of Ku-band scattering from the air-snow interface and motivation to retrieve the snow surface elevation from CS-2. Responses to the specific comments can be found below.

GC3: Even though Figure 6 and the interpretation is intended to stay qualitative (my guess), I strongly suggest to discuss these results in more detail. Putting more emphasis on increasing the credibility of the elevation estimates at this stage is very important in my eyes. You have the unique opportunity to have quasi-coincident air-borne and space-borne measurements. That's luxury and I have to admit that I am a bit disappointed that you do not exploit this luxury situation further. If I'd be allowed to recommend something, then I would i) quantify the temporal and spatial differences in the tracks and try to investigate whether a correction towards a better spatiotemporal match is worth an effort, ii) collocate the tracks with ice-type information (it might be sufficient to figure out where first-year ice and perennial ice was present), iii) collocate the tracks with meteorological information, e.g. from ERA-Interim or MERRA-2 or perhaps even from one of the higher-resolving weather forecast models to figure out whether air temperatures have been close to 0degC and/or whether and what kind of precipitation potentially occurred (Ideally you have a look at the meteorological conditions of not just the day of the coincident measurements but also of a 1-2 weeks period before to catch potential melt events and hence snow metamorphism near the air-snow interface.). See also my respective comments for Figure 6 and its interpretation.

You are correct that this comparison was meant to stay qualitative and be used simply as motivation for progressing to freeboard retrieval using this method. However, we realize it does provide a great opportunity to evaluate the retrieval and have addressed these points more in the revised manuscript.
We have collocated the tracks with meteorological information from MERRA-2 (both on the day of and 2 weeks leading up to the flight) and ice types on the day of the flight from the EUMETSAT Ocean and Sea Ice Satellite Application Facility (OSI SAF). Both flights took measurements over "first year ice" as noted by the OSI SAF. In the two weeks leading up to the flights, temperatures never rose above 0 deg. C, but did get relatively close (which would potentially indicate some surface melt and change in the surface backscatter). Also on both occasions, there was light snowfall 3-5 days before the flight, with rates staying below 5 mm/day.
The largest noticeable difference between the two dates is a strong north-south surface temperature gradient present during the 2011 flight, while the 2012 flight had near-constant surface temperatures along the flight line, shown in the revised figure 1.
Responses to the specific questions and detailed information on the meteorology leading up to the flight can be found in the revised manuscript and the replies below.

GC4: The interpretation of Figures 7 through 9 would also very much benefit from a more critical discussion which should also involve more work done by other researchers. I find a lack

of attempts to explain the differences observed, e.g. in Figure 9. See my specific comments to these figures.

The results were indeed lacking as far as explaining the differences observed, which could be improved by relating the results to work done by other researchers. To this end, we have added further comparisons with other works, including that of Schwegmann et al. (2016) and Paul et al. (2018) and revised the conclusion section. In reference to figure 9, we agree with your other comments on how this comparison is indirect (i.e. not overlapping in time and involves data coming from different time period lengths) and therefore refrain from giving much explanation of the differences observed or any real quantitative/statistical comparisons. That being said, we have added more explanation to differences observed between other overlapping measurements made from CryoSat-2, found in section 6.2.

Specific comments: Abstract: I suggest to add the standard deviation or Root-Mean-Squared difference in addition to the mean difference values given. If computed, also modal values of the difference would allow to give the obtained values more credibility.

Standard deviation values were added to the abstract. Modal values were computed and included with the figures in text, in Figure 7 and section 6.2, paragraph 1.

Page 1 L30: I guess, since you are focussing on Antarctic sea ice it would not hurt do use citations referring also to the albedo observed over Antarctic sea ice: Brandt RE, Warren SG, Worby AP and Grenfell TC (2005) Surface albedo of the Antarctic sea ice zone. J. Climate, 18(17), 3606–3622 (doi: 10.1175/JCLI3489.1) and Zatko and Warren, Annals of Glaciology 56(69) 2015 doi: 10.3189/2015AoG69A574

Agreed – We have removed the citation for Perovich et al., 2002 (which focused on Arctic sea ice) and replaced it with citations for Brandt et al., 2005 and Zatko and Warren, 2015, found in section 1.

Page 2 Line 2: I suggest to cite Comiso et al., J. Climate, DOI: 10.1175/JCLI-D-16- 0408.1 instead of Beitler 2014; the former is a peer-reviewed paper.

The reference was changed.

Line 6: Please add "Antarctic" or "Southern Ocean" to make clear that these shipbased observation based sea-ice thickness data set is valid there but not general in the polar regions.

Added "in the Southern Ocean".

Line 5-13: - Is there a reason why you refer to multiyear ice only for the Arctic? - Is there a reason why you refer to sea-ice thickness in the Arctic only while for the Antarctic you refer to sea-ice thickness in volume? Is the sea-ice thickness retrieval in the Antarctic more accurate so that it makes sense to also derive the volume?

Multi-year ice was referenced because the Arctic study (Kwok et al., 2009) estimated trends over multi-year ice alone, while in the Antarctic study (Kurtz and Markus 2012) did not discriminate. There was no intentional reason to mention sea ice volume in the Antarctic only, however, this paragraph was revised substantially and no longer includes these references alone (see introduction, GC1 above).

Line 14-20: - I am not sure I like the mentioning of Kwok et al. (2009) and Kurtz and Markus (2012) as the role models for sea-ice thickness measurements from active satellite sensors. Since you are basically referring to the principle, wouldn't it be sufficient to simply write what you wrote without these two references? I I guess my dislike comes from the fact that there have been earlier papers that describe how laser altimetry (which is the main focus in this paragraph) can be used to get an estimate of the total freeboard of snow-covered sea ice: Kwok et al. (2004) or Kwok et al. (2006) for the Arctic and Zwally et al. (2008) for the Antarctic.

The introduction has been revised. Zwally et al. 2008 (among other works) has been included for describing how laser altimetry can be used to retrieve total freeboard (see introduction, GC1 above).

L21-30: - I suggest to re-organize the sentences starting in Line 24 to avoid that sea-ice freeboard is used before being explained. How about you write along these lines: "... 2010-2012. The difference between laser ... [continue until Line 29] ... above the sea surface, known as the "sea-ice freeboard", and is used to calculate sea-ice thickness applying appropriate assumptions (see previous paragraph)."

Thanks for the suggestion – the introduction has been substantially revised and this sections has been changed. The freeboard is defined first, section 1 paragraph 2, and then used after that.

L31-39: - I suggest to expand rightaway in Line 31: "by the depth and variable vertical structure of the snow on top ..." - In Line 32, I suggest to add that it is not simply more precipitation but "... more and more frequent precipitation ..." - Line 34: "sea ice down near the" –> perhaps better: "sea-ice surface down near or even below the"
 - I suggest to break in Line 38 for a new paragraph, starting with "While ... ".

These suggestions have been made in the revised introduction.

- Is there perhaps also the chance that you quantify how large or weak the scattering at the air-snow interface is compared to that at the ice-snow interface? This could make your motivation stronger about why it might be reasonable to look for the snow surface scattering contribution even in Ku-Band.

This explanation is done in section 3 ('Observed Ku-band scattering of radar from Antarctic sea ice'). I've added "(discussed in section 3)" to page 3 line 17 for more clarification.

I strongly suggest to seek for evidence in the literature about the possible strength of the snow surface backscatter at Ku-Band (at nadir) to underline that it is physically reasonable to use CS-2 SIRAL returns for snow freeboard retrieval. I am stressing this because there exists literature in which one aims for snow-depth on sea ice retrieval by confidently assuming that Ku-Band penetrates to the ice-snow interface and combining it with a Ka-Band radar such as from SARAL AltiKa (Guerreiro et al., 2016). Your attempt is clearly conter-acting their assumptions.

We agree that more literature surrounding the strength of the snow surface backscatter at Ku-band needs to be referenced in this section of the manuscript. In particular, we have added Giles et al. (2008), which deals with CS-2 sea ice elevation retrievals in the Antarctic, and Willat et al. (2010), which shows that the strongest Ku-band return can come from either the snow surface, within the snow layer, or the snow-ice interface. More information on the backscatter from the snow surface is found in section 3.

We acknowledge that the dominant backscatter from Ku-band altimetry often occurs within the snow layer on Antarctic sea ice (Schwegmann et al. 2016 and others) and also that it is often approximated to penetrate to the snow-ice interface over Arctic sea ice (Geurreiro et al. 2016, Kurtz et al. 2014, and others). Here, we are introducing the fact that although the dominant scattering occurs below the snow surface, there exists some scattering from the air-snow interface (as shown in Willatt et al. 2010) that we can exploit for snow freeboard retrieval. In that regard, we do not believe we are directly counteracting the assumptions of Guerreiro et al., 2016 and other published works, but instead expanding on the utility of Ku-band returns.

Page 3: Line 10: "builds off" ?
Changed to "builds on".

Line 22: I don't understand the mentioning of the "originally 128". What is this for?
Removed.

Line 34-37: The motivation for choosing data from October is clear. You could have stated why you did not also use data from November. Most of the ICESat spring measurement periods last well into November. Here you state years 2003 to 2009 for ICEsat as years with measurements but actually using you are only data from 2003 to 2007. I can understand that the main motivation for this is to use the data produced by one of you. But from NSIDC and potentially also from University of Hamburg you could possibly have obtained ICESat freeboard data for 2003 through 2009, i.e. from an equally long period as you have CS-2 data from. You stated yourself explicitly, that "Seven years of data allows for a longer-term average to be computed"
We felt that because the comparison between CryoSat-2 and ICESat is (and will always be) indirect, that one month of data would be enough to compare to the spring ICESat campaigns. We agree that both months would be better, but feel one was adequate to assess the distribution. In the later years of the ICESat campaigns, the lower laser energy led to questionable freeboard retrievals, and therefore was not processed using this method. Again, we felt that with the indirect nature of this comparison, the time span chosen was long enough. We have, however, more explicitly stated the differences when discussing the results in the revised manuscript.

Page 4: Line 1: - It would be helpful for a better understanding of Figure 3 to mention the frequency range of the FMCW snow radar. - "First, ..." –> Where is the "Second"?
Added both suggestions to section 2, paragraph 4.

Line 8-12: Is this a gridded product? If yes, which grid resolution does it have and what is done to fill the gaps between the ICEsat overpasses?
Correct, it is gridded. This has been added to section 2, paragraph 5.

Line 13-16: You are using sea-ice concentration data obtained with the NASA-Team algorithm. While when choosing a 50% sea-ice concentration threshold is might not really matter which product to use there is published evidence that the NASA-Team algorithm often severely under-estimates sea-ice concentrations in the Antarctic compared to the truth - particularly in late winter / spring. You could avoid students and early-career scientists being trapped by your choice by choosing a more appropriate sea-ice concentration product right from the beginning, i.e. based on the ComisoBootstrap algorithm or the Eumetsat OSI-450 algorithm.

Thank you for pointing this out. In the revised manuscript, we have used the Comiso Bootstrap algorithm at the 50% threshold. This has been included in the datasets section (section 2, paragraph 6) and in the updated figures.

Line 18: "... altimetry tend ..." –> I suggest to insert: "for ice freeboard retrieval"
Added, thanks for the suggestion.

Line 20: You could cite Willat et al. (2011) here.
Added.

Line 35/36: "This result is expected, as it means that the scattering power from the air-snow interface is closer in magnitude to that of the snow-ice interface in snow radar returns" I do understand your conclusion from the smaller difference in power (about 13 dB for snow radar and 14 dB for Ku-Band altimeter) but I don't understand why this is expected. Lets assume for simplicity that the peak power is 20dB at the icesnow interface for both instruments. Then the power at the air-snow interface would be about 7 dB for the snow radar and 6 dB for the Ku-Band altimeter and with that the power at the air-snow interface would be SMALLER at that frequency from which you assume that the backscattering at the air-snow interface is LARGER. How does this fit together?
What is expected is that the power at the air-snow interface is larger for the snow radar than the ku-band altimeter. This is expected because the snow radar is often used to resolve the two interfaces and calculate snow depth. We do not assume that the air-snow interface power from the Ku-band is larger, but state that because it is similar to the snow radar, that we can expect to have scattering from the air-snow interface in the ku-band.

Page 5: Line 2: At the end of this paragraph interpreting Figures 3 and 4 I have a few questions.
i) How accurate are the two instruments with respect to the dB values shown?
The two instruments aren't radiometrically calibrated, so it is difficult to know the accuracy with respect to the dB values shown (Some radar parameters from each can be found in Panzer et al. 2013 (snow radar) and Gomez-Garcia et al. 2012 (Ku-band, conference paper)).
Along the flight lines presented here, the snow radar had a mean noise level of -29.1 dB (std:1.39 db) and a mean air-snow interface signal level of -16.8dB (std: 1.47). The Ku-band had a mean noise level of -30.3 (std:1.32) and a mean air-snow interface signal level of -17.9 (std: 2.09), showing that the return from the air-snow interface is well above the noise level in both cases. We have included these values in the caption of figure 3.

ii) How relevant is the similarity in the histograms shown in Figure 4 with respect to the shared mode at about 11dB while at the same time the histogram shows secondary modes at 16dB (snow radar) and 20 dB (Ku-Band).
The point of this figure was to show that the histograms are indeed similar to strengthen our case for tracking the air-snow interface from Ku-band. The shared mode is encouraging in that regard, while the secondary peaks could mean that the snow radar is more sensitive to resolving both interfaces when the power difference is larger between the two (as is expected, since the snow radar is used for deriving snow depth).

In addition I have a few comments: iii) What were the meteorological conditions during that flight? Can we expect homogeneous snow properties in terms of snow wetness etc.

iv) How would Figures 3 and 4 look for the October 2011 campaign? Would they result in the same result?

We would expect relatively homogenous conditions during the 2012 flight, judging from the surface temperatures (from MERRA-2, below) and the ice type (taken from EUMETSAT Ocean and Sea Ice Satellite Application Facility) which gives the same "first year ice" classification everywhere along the line.

MERRA-2 Surface Temperature
22:30UTC – 11/07/2012

Temperature (Deg. C)

−25.0 −22.5 −20.0 −17.5 −15.0 −12.5 −10.0 −7.5 −5.0 −2.5 0.0 2.5 5.0
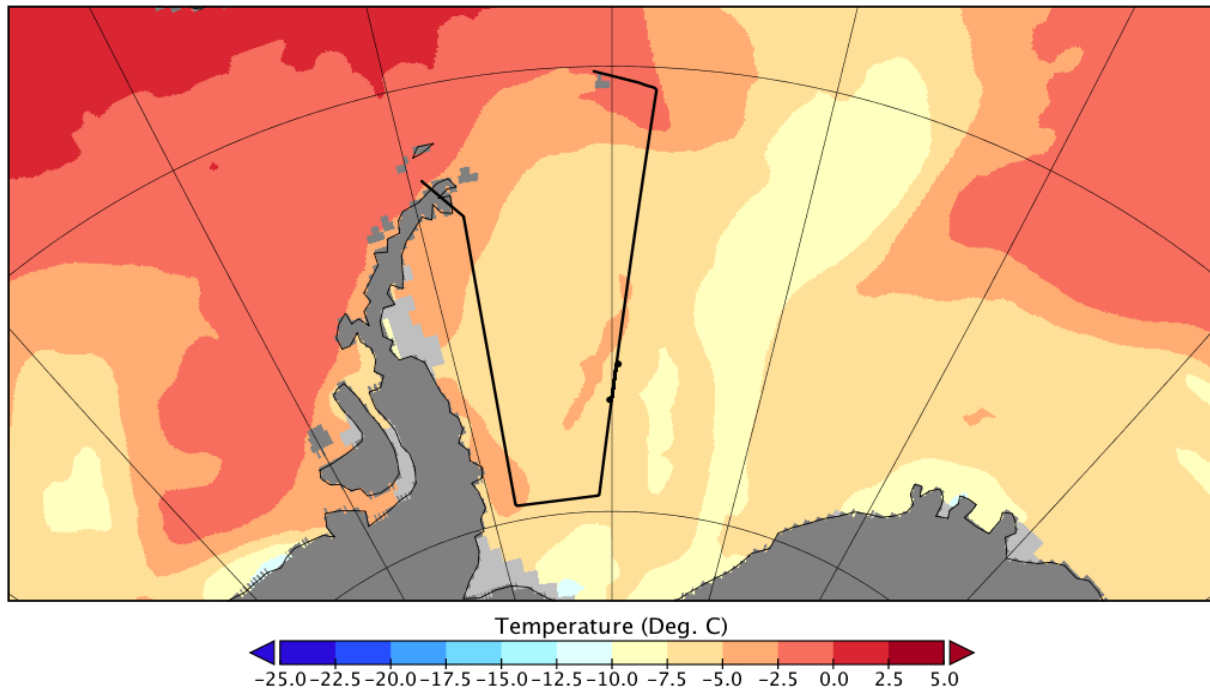
In 2011, the ice type was again classified as first year ice everywhere along the line, however, there was a stronger surface temperature gradient along the flight line (shown below). This gradient may have resulted in inhomogeneous snow properties that could have altered the radar returns. In this regard, figures 3 and 4 in the 2011 campaign may have looked slightly different than the 2012 campaign and could be responsible for features observed in figure 6.

MERRA-2 Surface Temperature
19:00UTC – 10/13/2011

Temperature (Deg. C)

−25.0 −22.5 −20.0 −17.5 −15.0 −12.5 −10.0 −7.5 −5.0 −2.5 0.0 2.5 5.0
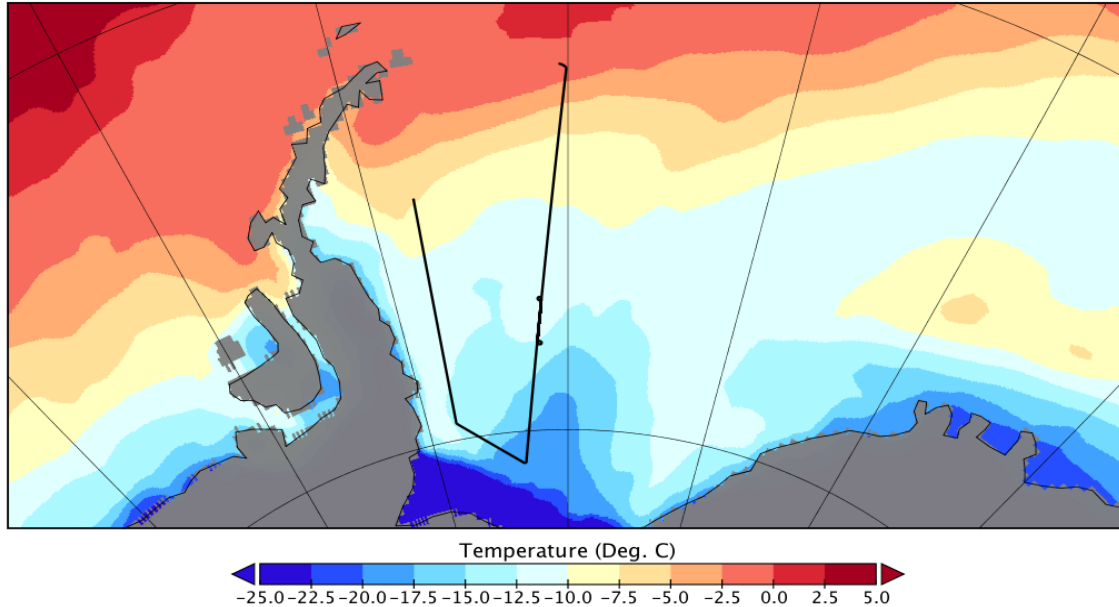
The meteorological conditions during these flights have been added to figure 1 and discussed (along with the ice types) in the revised manuscript, under the initial validation (Section 5).

v) What is the length (in kilometers) of the transect (or echogram) shown in Figure 3?
The echogram here is taken from a single datafile, which in this case covers just over 3km (3.016km). This has been added to the figure description.

vi) The Ku-Band altimeter histogram in Figure 4 has a substantially longer right tail with high dB values. It is almost certain that these values are responsible for the 1dB difference observed between the snow radar and the Ku-Band altimeter data. Are these particularly large differences the result of a particularly low power at the air-snow interface compared to the peak power or is this the result of peak powers being generally elevated at Ku-Band compared to the snow radar?
Agreed – the tail is likely responsible for the difference between the two observed. The differences between the histograms are probably a combination of both, since the snow radar generally has higher power at the air-snow interface (as it's used for snow depth retrievals) and also since peak Ku-band returns tend to be larger than peak snow radar. However, this figure was just meant to highlight the similarity in the histograms, which we feel it adequately does.

vii) What explains the larger time difference between the locations denoted by red and black points in Figure 3 for snow radar echogram compared to Ku-Band?
The snow radar tends to resolve the interfaces better, as can be seen in the more separate "interfaces" tracked by the peak-picker. The Ku-band, at a higher frequency, tends to be slightly less sensitive to the air-snow interface and also attenuated more by the snow volume, and thus has less-defined interfaces and smaller time differences.

viii) What is the source for the staggered echos above the air-snow interface at Ku-Band? Such echos are not at all present for the snow radar data.

These staggered echoes are returns from radar sidelobes, which are primarily a function of non-linearities in the transmit pulse. Over strong ice returns (seen in the figure) sidelobes can be present in both radar echograms, however in this case, the Hanning time-domain window filter applied to the data removed sidelobes from the snow radar but not the Ku-Band. Our peak-picker is designed to ignore staggered echoes such as these.

Line 21: What is "n"?
The variable "n" is part of the summation ($\sum_{n=0}^{N_b}$) and stands for each of the synthetic beams (N_b) in the sum.

Page 6: Line 2: I guess "thicker snow depth" and "scattering effects from the snow surface" are not as much linked with each other as scattering effects from the snow volume. What makes a thicker snow cover to have more surface scattering than a thinner snow cover?
This line was intended to mean that the entire snow layer (encompassing both the surface and volume) cannot be neglected. It has been rephrased to read "…scattering from the snow layer cannot be neglected…" to reduce confusion, section 4.1.

Line 27: Why "Though"?
Removed "though" and added "however" in the last paragraph of section 4.1, for clarity.

Page 7: Line 16: What is the motivation to only use a different initial guess for alpha in case resnorm is too high after the first fitting attempt?
The motivation to only use alpha comes from the fact that it is the least well-constrained initial guess variable, and that re-fitting with a new alpha tended to reduce the fitting error. While other initial guesses could have been modified and re-fit, we felt that it was not necessary due to the facts that a) they are all empirically derived and b) the added computation cost did not outweigh the benefit.

Page 8: Line 8: Are these PP and SSD thresholds also taken from Laxon et al. (2013)?
Yes, the PP and SSD thresholds are taken from Laxon et al., (2013) though there is scaling factor of 100 difference present in the PP. As the PP was not explicitly defined in Laxon et al., 2013 the values are calculated following from Armitage and Davidson (2014), and SSD comes from the CryoSat-2 product. These references have been added.

Line 12: "seasonal average freeboard datasets" –> perhaps better "datasets of the seasonal average total freeboard"?
Changed.

Line 15: A very good place to cite the paper by Kwok and Maksym, 2014 in J. Geophys. Res., doi:10.1002/2014JC009943
Added.

Lines 23-25: Please explain how the OIB data area used. Did you take data from both flights? Did you average over all valid points? What is meant by "respective surfaces"? Two final question at the end of this section: What happens in the special case of a snow free ice floe?

What happens in case of a wet snow surface, where penetration of the Ku-Band into the snow cover is almost zero?

Added some clarification to this paragraph. Data were taken from the Ku-band radar from both flights, and the values found were the average of all valid points. The "respective surfaces" refer to the surface backscatter coefficients of the air-snow and snow-ice interfaces.

As far as the cases you mentioned: From CryoSat-2, it depends on the return waveform parameters (PP and SSD). In both of these cases, the return may be more specular than a typical snow-covered floe and be non-classified or classified as a lead. The chosen thresholds tend to limit misclassifications, but as with any retrieval process, misclassifications can still occur. We have added some more verification figures (5 and 6) to show how the algorithm performs over different regions and surface types.

Line 32: "found" –> perhaps better "computed" or "derived"?

Agreed, it has been changed to "derived" in section 5 paragraph 1.

Page 9: Lines 7-13 & Figure 6: - Please provide a measure of the total distance along the tracks shown in Figure 6 a) and b). This would make referencing to certain feature more easy in addition to simply providing an easier interpretation of the spatial scale we are looking at. - I suggest to add a vertical line at zero difference ATM minus CS-2 in images c) and d). - What is the average difference in successive measurements in images a) and b)? - Suggest to use the same y-axis scaling for a) and b) for a better visual comparability of the elevation variations.

The suggested changes have been made to figure 6. Instead of showing the lat/lon for each X axis tick, only along track distance is shown to reduce clutter and improve visibility. The starting and ending lat/lon pairs are included in the figure caption.

The distance between successive measurements is 0.38km (corresponding to the along-track footprint of CryoSat-2).

- I'd say that the overall agreement, i.e. the large-scale agreement is better for 2011 than 2012. - For 2011 the mean is very close to zero, right. But the modal value is between 5 and 10 cm with CS-2 underestimating ATM elevation. - CS-2 elevations quite often exhibit strong variations in magnitude; in 2011 more during the first third of the track, in 2012 during the first two thirds of the track. These strong variations (or jumps) are as large as about 40 cm and except in one case do not have a counterpart in the ATM elevations. Please try to give an explanation to these.

We believe these jumps are a product of the threshold chosen to represent "good fits" in the retrieval process. Currently, we use a residual value ('resnorm' in text) of 0.3 as the cut off for acceptable waveform fits. Fit waveforms with larger residuals are not included in the retrieval. When they are included, we see more points with anomalous elevation (i.e. more jumps). Lowering the threshold below 0.3 does help to remove some of the jumps, but also removes non-anomalous points and results in worse overall agreement between CS-2 and ATM. Therefore, we still find 0.3 to be the most appropriate threshold, and understand that the jumps are caused by "bad" fits that are still within our threshold of being "good". An explanation has been added to the text, section 5 paragraph 3.

- While in 2011 the large-scale agreement is quite good (you could even stress this impression by adding elevation profiles with largescale smoothing applied), in 2012 there appears to be a

systematic under-estimation of the ATM elevation by CS-2. Please try to give an explanation to these as well.

This potentially comes from the smaller footprint size of ATM compared to CS-2. ATM is able to resolve small-scale peaks that would get washed out in the CS-2 return. While it is not as apparent in 2011, there still exists a slight underestimation of ATM by CS-2 in the last third of the profile. This potential explanation has been added to section 5, paragraph 3.

- You argue that differences between the two elevation data sets might be caused by "initial temporal and spatial discrepancies between the two data sets. Would you be able to quantify these differences? Would it make sense to do a correction of the track of one sensor with respect to the track of the other sensor?

The discrepancies mentioned here mainly refer to the sampling differences between the two instruments, which would be difficult to quantify. The CS-2 footprint is around 1.6km across track and 0.38 km along track, while the ATM icessn footprint is much smaller (~250m across and 30m along). This itself would lead to different ice being sampled between the two instruments, and very likely different mean elevations per shot.

From this initial validation effort, we felt that the agreement was good enough to justify a freeboard calculation, and that performing a correction (for drift or footprint size) wouldn't factor into the freeboard retrieval, and therefore did not include it in this study.

- You write that both datasets "appear to detect similar locations of troughs and ridges along the flight line". I don't find this statement particularly convincing because there are also many cases where troughs in one dataset and ridges in the other dataset coincide.

Agreed. This statement has been removed from the text.

Lines 19-33: - Line 25: "fewer than five data points" –> What is the distance of successive data points? How many data points would fall into one 25 km grid box at maximum, i.e. diagonal crossing? Can you comment on the data density as well? How many CS-2 overpasses or days with CS-2 overpasses in one grid cell do you have in one month?

Each successive CS-2 point is .38km, which would result in a potential maximum of about 93 data points per orbit. The number of data points in each grid cell varies greatly depending on month and location relative to the continent. Values range typically from 0 (furthest north) to over 200 (further south, with multiple orbit passes over certain cells) raw data points. After filtering and removing anomalous freeboard measurements, around 58% of the initial waveforms remain. We have added figure 5, which shows this valid waveform fraction on a pan-Antarctic scale.

Lines 29/30: "Any points within each grid box ..." –> Could it be that this sentence should be placed before the previous sentence? I am asking because the previous sentence already describes the method used at grid level.

We are updating our freeboard calculation following comments from the other reviewer. This sentence has been removed.

– Line 32: "are smoothed" –> Why is this? Why do you do that? Is it because of the gaps between the overpasses? Please state so in the paper.

This is done mainly to reduce noise but also to fill gaps in the data. There are some gaps in the data between the overpasses and in grid cells that have been filtered out.
The following sentence has been added to the end of the paragraph: "Smoothing is applied to reduce noise in the CryoSat-2 data and also to fill in gaps in the data." (section 6.1, paragraph 1).

Page 10 Paragraph ending in Line 7: - While there is not too much work yet about freeboard distribution from radar altimetry in the Antarctic I still suggest that you consider comparing your results with the results published by Giles et al. (Geophys. Res. Lett., 2008), Schwegmann et al. (Annals of Glaciology, 2015), and Paul et al. (TC, 2018). - While the work of Nghiem et al. (2016) is really interesting and certainly not invalid over parts of the Antarctic MIZ I suggest that you also take into account (and at least mention if not discuss) the potential effect of ocean swell, lower CS-2 data density and hence a larger representativity error, and ice types being different in the MIZ than in the pack ice; a large fraction of the Antarctic MIZ is formed by the often several hundreds of kilometers of pancake ice or cake ice or first-year ice with small floe sizes (< 100 m) for which I doubt that CS-2 is going to provide reasonable elevation and hence freeboard estimates.
We have added many references that were lacking in the original manuscript, and our results have also been compared qualitatively to the freeboard distributions shown in Schwegmann et al. (2016) and Paul et al. (2018), in section 6.2.
Additionally, we have expanded our explanation of the ice edge in the revised manuscript to include effects of ocean swells and surface waves as well as the lower CS2 data density and differing ice types in the MIZ. This can be found in section 6.1, paragraph 2.
Figure 5 shows valid waveform fractions (as well as lead /floe fractions). Over the MIZ, there is a higher number of invalid waveforms (speaking to the complex ice types found here) that are not included in the freeboard calculations.

- I note that the distribution of total freeboard shown in Figure 7 is quite patchy and contains several artificial south-north oriented freeboard variations (possibly caused by sampling issues). I note that the freeboard in the southern Ross Sea is indeed lower than further north. However, given the fact that this is an area of extensive new-ice formation and export paired with low precipitation and hence thin snow cover, the freeboard values shown are certainly at the higher end of what is typical there - if not a proper overestimation. Sea-ice thicknesses in the southern Ross Sea are 20 to 50 cm ... total freeboards (without snow) therefore in the range of between 2 and 5 cm and not between 10 and 20 cm as indicated in the maps.
We have updated our freeboard calculations (to include on orbit filtering, at the request of the other reviewer) and thus the distribution differs slightly in the areas mentioned. However, the total freeboard is heavily dependent on the snow depth, which (even if it's small) is unknown. Also, these total freeboards in the Ross Sea do compare reasonable well with that found using ICESat in this region, and are similar to what is shown in Schwegmann et al. (2016) and Paul et al. (2018). Since there is no or little snow, the total freeboard should be close to the radar/ice freeboards. The added figure 5 shows that more lead-type waveforms are found in the Ross Sea, meaning fewer floe points are used to calculate freeboard than in other areas, which could explain the slightly higher-than-average freeboard values shown here.

Lines 8-15 & Figure 8 - "smallest measured freeboard" –> perhaps better "smallest measured mean October freeboard"

Changed.

- 25.77, 27.6, 12.97 ... I suggest to give these figures with the same number of digits, i.e. 25.8, 27.6 and 13.0.
Changed.

- Showing the mean total freeboard together with the sea-ice area is certainly fine even though, as you stated correctly, it is not too clear why you find a good correlation between these two quantities. However, instead of the sea-ice area one could plot other variables as well. One would be the standard deviation of the mean total freeboard as a measure of the scatter of the mean values. A second one would be to show either the number of 25 km grid resolution grid cells with valid CS-2 data or even the number of individual valid freeboard (or elevation) measurements. Since you have many gaps in the original CS2 data it would potentially be a very interesting additional information. - I note that the maximum inter-annual difference of the mean October freeboard is 2 cm. Is this within or outside the retrieval uncertainty?
We definitely agree that we could plot different variables here, however, the point of the figure was not meant to be further validation of the algorithm, but instead to simply show that a relationship may exist and could be explored further. We have added additional figures / information throughout the manuscript that act to further validate the performance of the algorithm. More coincident measurements are needed to fully quantify the uncertainty in this method, something that will be done in future work.

Lines 17-25 and Figure 9: - I suggest to color the open water in a grey tone (different than Antarctica of course) to ease discrimination between areas with differences close to zero and open water. - I suggest to reduce the range of the differences shown to +/- 30 cm to show more details. The way the range is chosen currently only reflects the larger differences.
We have revised this figure to account for these issues, but instead changed the color bar to include grey instead of white (Figure 10).

- I find it essential that you mention three things in your discussion of this Figure: i) the larger number of years for CS-2 (7 instead of 5), ii) the fact that the ICESat data cover different time periods with at least 2 of the five years have a substantial if not dominating overlap in time with November and hence conditions changed towards spring (As far as I recall you analysis you did make the effort the average CS-2 from exact those dates from which also ICESat measurements exist.), iii) the fact that we look at years 2011-2017 for CS-2 but 2003-2007 for ICESat, i.e. two different, not overlapping time periods. While this might not have an effect it needs to be stressed once more in the context of this discussion. Finally, iv) one could ask whether you used the same method for averaging the CS-2 data (and filling gaps, extra- or interpolating gaps) than was done in Kurtz and Markus, 2012? Because of these four issues I warmly recommend to delete the last sentence in Lines 24/25.
We tried to emphasize that these were not direct comparisons, but agree that more could be added to fully explain the differences between the two datasets. We used the same method for averaging and filling gaps as was used in Kurtz and Markus (2012), however with an updated freeboard calculation, the averaging has been done slightly different in the revised manuscript, though the gap filling has remained consistent.

These points have been added to the description as its own paragraph (section 6.2, paragraph 2) and the last sentence has been removed.

 - When talking about a difference of only 1.9 cm: What are the uncertainties in monthly mean freeboard from CS-2 and from ICESat? Is the difference about the uncertainty?
The estimated uncertainty in the ICESat freeboard is 1.8cm (Kurtz and Markus, 2012). Unfortunately, freeboard from the IceBridge underflights in the Antarctic have not yet been processed by the OIB team, and therefore no coincident "true" values exist from which to calculate uncertainty. Future work will compare freeboard calculations directly to better characterize the uncertainty in this method.

 - You do not make any attempt to explain the highlighted negative freeboard differences CS-2 minus ICESat in the Weddell and Amundsen Seas. Why?
This has been inadvertently left out of the original manuscript. It could be due to a number of reasons, however, since the time periods of data from ICESat and CryoSat-2 do not overlap, differences observed aren't necessarily due to discrepancies in retrievals (i.e. both methods could both be showing the "true" freeboards). Therefore, we tried to refrain from explaining differences from ICESat. We add some explanation of differences seen between our method and the works of Schwegmann et al. (2016) and Paul et al. (2018), found in section 6.2, paragraph 3.

- How do your results compare to the work of independent researchers: Yi et al., 2011, Kern and Spreen, 2015, Kern et al., 2016, Li et al., 2018?
Instead of comparing our results to more studies that use ICESat data, we have instead elected to compare our results to studies using CryoSat-2, to see how the freeboard distribution compares to other radar-based products. Specifically, we have qualitatively compared our results to Schwegmann et al. (2016) and Paul et al. (2018), found in section 6.2.

Lines 27-36, Figure 10: - Figure 10 is indeed quite interesting because the highest "snow depths" are not observed in the Weddell Sea but on East Antarctic sea ice. Puzzling. This is even contradicting your own work (Kurtz and Markus, 2012), where the freeboard maps shown are assumed to represent the snow depth while assuming sea-ice freeboard to be zero. In that work maximum freeboard and hence "snow depth" was observed in the Weddell Sea. What is further interesting is that the "snow depth" is nowhere considerabler smaller than 10 cm - even not in the southern Ross Sea where there is little or no snow on the young sea ice. - I would have found it again very useful, if you would have related the results shown in Figure 10 also with other work, i.e. snow depth based on satellite microwave radiometry (Markus et al., various) or based on ICESat data (Kern and Ozsoy-Cicek, 2016).
We didn't compare these retrieved "snow depths" to other sources, since we believe the snow-ice interface is not being tracked well in this algorithm, and thus these results do not accurately represent the actual snow depth distribution. Further work will need to be done to improve the retracking of the snow-ice interface to retrieve snow depth, if indeed it is possible given the attenuation of the radar signal in flooded/briny snow.

Page 11: Lines 1-4: That the peak-picking algorithm provides snow depth along that flight line which is within 10% of the values published by Kwok and Maksym (2014) is an encouraging result and should be highlighted more.

We agree that it is indeed encouraging, but have done little in the way of close verification of the interface detection for each data file along the flight path. We feel it is best to refrain from highlighting this result until more validation is done.

Lines 4-6: I am pretty sure that this is a frequency issue and not an issue of bandwidth or footprint size: The snow radar used on OIB is a 2-8 GHz radar, right?, while CS-2 operates in Ku-Band.
With the "correct" snow conditions it is very likely that CS-2 does not penetrate down to the ice-snow interface, explaining the considerably lower "snow depth" value estimate from the two elevations. Actually, the OIB snow depths are potentially even higher because of the difficulties to retrieve snow depth in areas of deformed sea ice and on multiyearlike ice reported elsewhere.
You're correct that CS-2 likely does not penetrate down to the snow-ice interface, and this is something we included in explanations in the previous paragraph. Assuming that CS-2 is tracking the correct snow-ice interface (as other works have done) we would still expect the snow radar-derived snow depth to be larger due to the footprint size and bandwidth discrepancies between the two instruments.

Comment: Again I doubt that the precision and accuracy of the data warrants to give mean values with 3 digits = millimeter precision here. I guess 0.29 m, 0.26 m and 0.15 m would do it.
Changed.

Line 8: I suggest to delete "slightly". It is considerably greater.
Removed "slightly".

Line 12: "validating" –> perhaps better "evaluating" or even only "understanding".
Changed to "evaluating".

Line 13: "to better understand the snow depth distribution on sea ice" –> perhaps better: "to use it together with the air-snow interface for snow depth on sea ice estimation."
Changed.

Lines 15-27: - Line 16: "air-snow interface of sea ice" –> perhaps better "air-snow interface of snow on sea ice".
Included "snow on".

- Line 20: "validate" –> "evaluate"
Changed.

- Line 24: "data from comes from" ...?
Removed the first instance of "from".

- Line 22-27: I strongly suggest you revise these conclusions based on the additional analysis, interpretation and discussion that is recommended in the general comments. In particular, figures for standard deviation and potentially also uncertainties should be given in addition to the mean values. One can have a mean value close to zero with one part of the data pairs having -50 cm difference and the other part having +50 cm difference ...

The conclusions have been revised based on the changes mentioned in these comments, especially adding the standard deviation values from these differences and reflect the updated freeboard calculations, figures, and comparisons to other sources.

Lines 28-33: - Line 28: "retrieved ice freeboard" –> you did not really retrieve ice freeboard, did you? You computed the snow depth from the difference between air-snow interface elevation and snow-ice interface elevation.
Correct. This was changed to refer to the retrieved snow-ice interface elevation values.

- Line 29: "lower than typically expected" –> since you did not show any other results about snow depth on Antarctic sea ice - expect for the case of East Antarctic sea ice - it is difficult to follow this statement.
The "lower than typically expected" was broadly referring to other studies that measured snow depth on sea ice, though a citation was missing from this manuscript. The revised manuscript includes a reference to snow depth measurements made from passive instruments (Markus and Cavalieri, 1998) and in situ surveys (Massom et al., 2001).

– Line 31: I agree about the potentially wide-spread flooding of Antarctic sea ice but sea ice is mostly flooded when the ice-snow interface is submerged be low the sea level and in that case an ice-snow interface does not exist in that sense anymore. If it still exists, e.g. through to lateral flooding it is possibly close to zero. It might therefore be more correct to again refer to sea water and brine wicked up into the snow, creating a saline snow - non-saline snow interface which is possibly the interface seen by Ku-Band.
Agreed, we have revised this section to mention the brine layer that is likely detected in the Ku-band (section 7, paragraph 1).

Question: For the location of the air-snow interface you have a-priori information from seasonal mean ICESat snow freeboard. For the ice-snow interface you don't have any a priori information, do you? This could be one explanation for the sub-optimal performance with regard to detecting the ice-snow interface as well.
This could be one explanation for the sub-optimal performance, yes. Another could be the fact that although the threshold retracking used here has shown to be successful at retrieving the snow-ice interface in other works (Laxon et al., 2013; Kurtz et al., 2014) the addition of more free parameters could lessen the usefulness of the threshold chosen for snow-ice interface tracking.

- Line 34: I guess it would be fair to cite the already existing literature about using CS-2 data for Antarctic freeboard (sea-ice thickness) retrieval: Paul et al., 2018, and change "... observing Antarctic sea ice." into something like: "... observing Antarctic sea ice with satellite radar altimetry in addition to Paul et al. (2018)." Maybe there is even more work out using CS-2 data in the Antarctic? Please check!
We have revised the conclusions to include the Antarctic freeboard retrievals made by other authors (Schwegmann et al., 2016; Paul et al., 2018), and focused on the novelty of retrieving snow freeboard (as opposed to ice freeboard) from CS2.

Page 12, Line 7: Again I think it would not be too bad to add the work of other authors here to avoid the impression that you are the first on this field: "... for improved retrievals of Antarctic sea ice thickness, complementary to sea-ice thickness retrievals based on the 15+ years long time series of combined Envisat - CryoSat-2 freeboard estimates (Paul et al., 2018)."
We have included the work done by ESA's CCI Sea Ice group (Schwegmann et al., 2016; Paul et al., 2018) in this statement, to exemplify how long time series of sea ice freeboard and thickness can improve understanding of sea ice overall.

Page 23: Line 23: Giles et al. This paper was in Geophys. Res. Lett. and not The Cryosphere
Changed – thank you.

Reviewer 2 (Stefan Hendricks):

In their paper "Retrieval of snow freeboard of Antarctic sea ice using waveform fitting of CryoSat-2 returns", the authors develop and apply an algorithm to obtain snow freeboard of Antarctic sea ice using waveform fitting of CryoSat-2 data. The waveform fitting is based on a forward model from earlier work of one of the authors and the main work here has been the to include backscatter from multiple interfaces (air/snow and snow/ice) in combination with snow volume backscatter for the application of sea ice in the southern hemisphere with its higher and more complex snow load. The authors compare the results with airborne validation data and earlier ICESat laser altimeter results and conclude that their algorithm can be used to obtain snow freeboard with the CryoSat-2 during the maximum austral sea ice extent in October. They also investigate the potential to retrieve snow depth from CryoSat-2 waveforms, but do not find realistic results except for an area in the East Antarctic sector.

I have been part of the team that produced freeboard maps of Antarctic sea ice from Envisat & CryoSat-2 data in the Climate Change Initiative. We used an empirical retracking scheme, which made it difficult to include the contribution of snow backscatter in the freeboard algorithm without prior knowledge of its impact on waveform shape. We are acutely aware of this deficiency in the CCI sea ice thicknesses for the southern hemisphere, and it is commendable that the authors attempt to overcome this issue. Therefore this study is for me a very welcome and novel contribution to the field of remote sensing of Antarctic sea ice thickness. The concept is generally sound, but there are a number points that need to be addressed before publication. I have detailed my concerns in the general and specific comments below:

We would like to sincerely thank the reviewer, Stefan, for his important and insightful comments on this manuscript. The insight he shared from his own experience with CCI Antarctic sea ice freeboard retrievals certainly helped to improve the quality of this retrieval method. Our responses (in blue) to each of the comments (in black) can be found below.

General Comments:
1) It is understandable that maps of snow freeboard is the main objective of this work, but the authors show very little in terms verification of the different algorithm steps. The waveform fitting is based on nine free parameters, but it is not clear to me what the sensitivities are for resolving the snow backscatter properties. E.g. do snow backscatter/depth and surface roughness have an ambiguous impact on waveform shape and thus range? In general, the potential impact of surface roughness changes receives very little attention in the evaluation of the results. The fact that the snow depth resulting from the waveform fitting is unrealistic in wide parts of the study regions shows that there are issues with fully resolving the backscatter processes. A sensitivity study of the waveform forward model would help greatly to assess the skill of the algorithm for different snow conditions. Regional information on the average waveform fit quality would also be of interest to the reader as it might help to identify issues of the algorithm. I find this especially important as the direct validation with the

Operation IceBridge ATM and snow radar data is very limited compared to the spatial and temporal extent of the CryoSat-2 data and the otherwise indirect comparison to ICESat.

We realize the original manuscript was indeed lacking in the verification of the sub-steps of this retrieval method, and have added additional figures and information throughout the revised manuscript.

The impact of surface roughness on the results was not discussed because we felt the impact would be small for our objective, which is simply to show the possibility of this technique to derive snow freeboard. Additionally, surface roughness is not explicitly handled by the model, but instead, backscatter values are taken from an initial guess and derived through the waveform fitting process. We acknowledge that surface roughness does play an important role on the backscatter properties, but it is one that will be explored in future work aiming to improve the accuracy of this algorithm. The revised manuscript will mention this fact. Waveform fit quality will also be made apparent in the revised manuscript, focusing on goodness of fit distributions across the sea ice pack as well as a discussion of the percentages of waveforms that are filtered out in this process (revised figure 5, below). Surface type classification fractions will also be included to better assess the performance of the algorithm. See specific comments below for more details.

2) The conversion of surface elevations into snow freeboard is not state-of-the-art, in parts problematic and the authors risk to undermine the value of their retracker development work. For example, the authors use a surface type classification scheme that was originally designed for Arctic sea ice and an earlier version (baseline-b) of the CryoSat-2 Level-1 data. For the ESA CCI data set we had to define separate waveform parameter threshold for Arctic and Antarctic sea ice. The authors need to show that there is no preferential sampling of surfaces that may introduce a freeboard bias, which can be easily done by providing information on detection rates for lead and floe surfaces and compare those the surface type fractions of the ESA CCI dataset (Paul et al. TC 2018). I would also strongly suggest to compute freeboard per orbit and not by subtracting monthly mean elevations and sea surface height. In our experience the geophysical range corrections in the CryoSat-2 Level-1 product files are not good enough for this approach. Using the instantaneous sea surface height during the orbit will be more reliable and also yield better options for filtering incorrect retrievals.

It is acknowledged that the lead/floe classification scheme used here was originally developed for the Arctic which deserves further analysis, however since our methodology maintains the same 128 bin sampling as the Baseline B data there should be no difference with regard to product version. In the added verification steps, we have shown detection rates for the lead/floe classification scheme, shown in the revised figure 5:
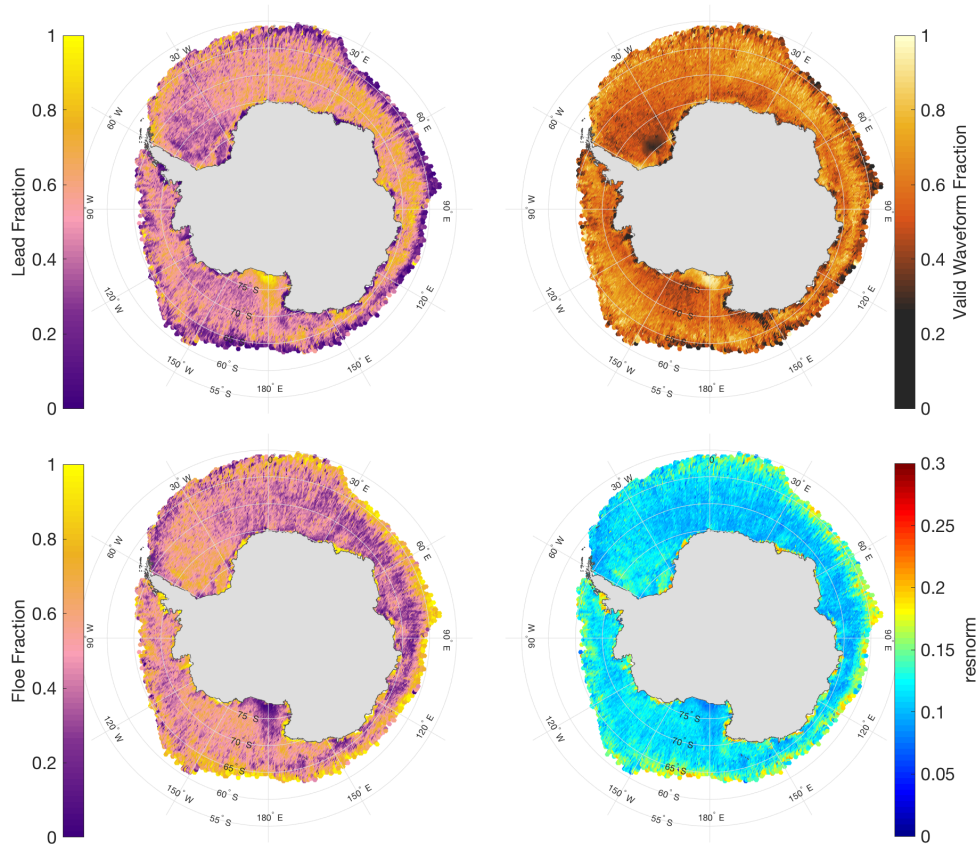
There are some differences from Paul et al. (2018); here, there appears to be a smaller sea-ice-type waveform fraction overall and specifically a greater concentration of lead points in the Ross Sea as compared to Paul et al. (2018). It is likely that this method is classifying smooth, new ice in the Ross sea as lead points – a fact that is discussed in the revised manuscript. The maps above are from October 2016 while Paul et al. (2018) has maps from September 2011, which could be a potential source of the differences observed. A more detailed discussion has been included in the revised manuscript, Section 4.3.
In addition, we have updated our calculations of freeboard slightly to include on-orbit filtering, which is explained below and in the revised manuscript, section 6.1.

3) Several earlier studies and datasets that are highly relevant for this topic are not mentioned and the manuscript gives the wrong impression that the work of the authors is the first application of CryoSat-2 for Antarctic sea ice. The authors also state that the impact of snow backscatter on ranging with Ku-Band frequencies is "often ignored" which I certainly do not agree with. It might be a matter of wording, since most operational CryoSat-2 products use the assumption that the freeboard is the average ice freeboard within the footprint. But this is due to the challenges of parametrizing snow backscatter and its temporal and regional variability, not the lack of awareness in the scientific literature. I have suggested references in the specific comments below. The

lack of reference to existing publications that specifically deal with CryoSat-2 freeboard retrieval in the southern hemisphere (Schwegmann et al, 2016, Paul et al, 2018) is also unfortunate, as these are a good motivation for this study. There would be added value if the authors compare their snow freeboards to the freeboard information in the ESA CCI CryoSat-2 data set (see data availability in Paul et al. TC 2018) and demonstrate the improvements and limitations of using waveform fitting.

We agree that the original manuscript was lacking in terms of references to published literature on the topic. The introduction has been completely revised to include recent applications of satellite altimetry to Antarctic sea ice, referencing Giles et al. (2008), Schwegmann et al (2016), Paul et al. (2018), and others. We have also revised other parts of the manuscript to make it more clear that the state of the science is well aware of the impact of snow backscatter on ranging from Ku-band and is not simply ignoring this fact. A comparison of the retrieved freeboard to that from Paul et al. (2018) would indeed be useful and has been included in the revised manuscript, in section 6.2. Additionally, we have revised the conclusions (section 8) to make it more clear that this is not the first application of CryoSat-2 for Antarctic sea ice, and instead stressed the novelty of retrieving snow freeboard from CryoSat-2.

Specific Comments:
P2L7: I guess you mean "active" in the sense of active microwave sensors respective altimeters in general? I would recommend to use the term "satellite altimeters" instead of "active platforms" throughout the document. (Typo: remove -> remote)

The "active" was intended to be in contrast to the "passive instruments" mentioned in the previous paragraph, but admittedly added some confusion. All mentions of "Active" instruments and platforms have been changed to "satellite altimeters".

P2L27: Typo: "of off"

Corrected to just "off".

P2L28: Beaven et al. 1995 states that the snow/ice interface is the dominated backscatter source. To my knowledge Beaven itself does not imply that cold snow under laboratory conditions is completely transparent for Ku-Band. This is a fine distinction but relevant for this paper.

Agreed, this is a necessary distinction to make for this work. The intro has been revised, and the new sentence reads "Most radar altimeters operate in the Ku band at around 13.6 GHz, a frequency that has been shown to produce a dominant backscatter from the snow-ice interface (Beaven et al., 1995)."

P2L39: Please rephrase the term "often ignored" as it does not properly reflect the state of the scientific literature. The issue is not lacking awareness of the importance of snow interface or volume backscatter for Ku-Band freeboard retrieval (e.g. Armitage and Ridout GRL 2015, Ricker et al. GRL 2015; Nandan et al. GRL 2017), it is the challenge of getting the temporal and spatial variability from the available waveforms. A better description would be "often not included freeboard retrieval algorithms, especially those depending on an empirical waveform evaluation".

That is better, thank you. We have revised this line to match the suggestion and included the appropriate references.

P3L30: The inverse barometric correction is included in the dynamic atmosphere correction. Both corrections should not be applied in combination.
Thanks for pointing this out, it was an error in the text as only the dynamic atmospheric correction is applied. For accuracy/clarity, the sentence has been changed to read "Geophysical corrections are applied by using the CryoSat-2 data products, which include the ionospheric delay, dry and wet tropospheric delay, oscillator drift, dynamic atmosphere correction (which includes the inverse barometer effect), pole tide, load tide, solid Earth tide, ocean equilibrium tide, and long period ocean tide."

P4L18: See comment above. There are several publications that investigate the impact of snow on CryoSat-2 freeboards and are not cited here.
We have added citations to a number of works that were missing from the original manuscript, and acknowledged recent studies dedicated to investigating the effects of the snow layer on Ku-band ranging and freeboard retrievals to the beginning of this paragraph. This includes references to Armitage and Ridout (2015); Ricker et al. (2015); and Nandan et al. (2017).

P7L7ff: At this point it would have been good if the authors had included a sensitivity study using their forward model. It is difficult to assess the skill of the waveform fitting if e.g. the impact surface roughness changes and snow backscatter on the waveform shape could be ambiguous.
Agreed – here we added a study (Figure 6) looking at the initial guesses for the standard deviation of surface height and the total backscatter, showing modeled waveforms, fit waveforms, and the corresponding freeboard maps (shown as a difference from the parameters chosen in the rest of the study).
It is important to note that surface roughness is not explicitly included in the current form of the model, as we feel the impact of surface roughness will not affect our goal to show that snow freeboard retrievals are possible with CS-2. Surface roughness changes are important and will surely need to be taken into account in order improve the accuracy of the retrieval method, but this is something that will be done in future work.

P7L22ff: The authors should provide information on the detection rates for lead and ice surfaces. In Paul et al 2018 (TC) we needed to introduce different waveform parameter thresholds for Arctic and Antarctic sea ice. There is a risk of introducing freeboard biases if the surface type classification is not performing well (Schwegmann et al. TC 2016).
Thanks - we have included this in figure 5. Overall, the distribution of leads and floes is generally comparable to that found in Paul et al. (2018), though differences are discussed in the text. Additionally, we have included the percent of valid waveforms, as well as the average resnorm value over the study period (October 2011-2017).

P7L30: The values for PP in Laxon et al. 2013 are: PP < 18 (not 0.18) and SSD <

4. I assume that the value of 0.18 is only a typo in the manuscript. But the issue that these thresholds are valid for an older version (algorithm baseline-b) of the CryoSat-2 Level-1 waveform. The authors must use baseline-c data for the later years of their data record and waveform oversampling introduced in this version changes pulse peakiness values. The authors should therefore verify their lead and ice detection rates (see above).

The PP and SSD thresholds are taken from Laxon et al. (2013), though there is a scaling factor of 100 difference present in the PP. As the PP was not explicitly deifned in Laxon et al. (2013), the values are calculated following Armitage and Davidson (2014). (This citation was included on P7L27 but not on P7L30 nor P8L8 – this has been corrected in the manuscript, section 4.3). Following Kurtz et al. (2014), we have resampled the baseline-c data so that each data type (SAR and SARin) are consistent with 128 range bins per shot. See above for lead/ice detection rates.

P8L8: Same PP threshold magnitude inconsistency. Laxon et al. 2013 reports PP < 9 and SSD > 4 as criteria for sea ice surface returns.

See answer above.

P8L33ff: Does this mean that the authors have removed the DAC and tides from the CryoSat-2 derived elevations and then applied a consistent DAC, tide and mss correction for both ATM and CryoSat-2? What about the inverse barometric correction (see comment above)? This approach however still leaves the ionospheric and tropospheric corrections as an uncertainty factor, which may a dynamic range of 10 cm or more (Ricker et al Remote Sensing, 2016) thus a non-negligible magnitude. A second validation in form of along-track freeboard might help to improve the initial validation.

To make the absolute elevation comparison, we are following the method put forth by Yi et al. (2018), which "…replaced the ocean tide, ocean loading tide, and the inverse barometer correction used in the CryoSat-2 Baseline C data product with ocean tide, ocean loading tide, and dynamic atmospheric correction…". Yi et al. (2018) was not published at the time of submission, but has since been cited in this manuscript. This was done to have consistent geophysical corrections between the CryoSat-2 and ATM data. The ionospheric and tropospheric corrections from the CryoSat-2 data product were applied.

An along-track freeboard comparison would help to improve the initial validation, however, IceBridge freeboard from these campaigns has not yet been processed by the OIB team. We have added the correlation coefficients and further explanation to this paragraph, section 5.

P9L19ff: Filtering waveform is standard practice. The question is how many are filtered out?

This filtering method results in the filtering of just under 42% of the total number of waveforms. The average valid waveform fraction is .5832, which has been added to this paragraph in the manuscript, section 6.1.

P9L24f: The practice of computing freeboard by subtracting monthly means of sea surface heights and surface elevation is definitely not state-of-the-art. It puts a lot of trust in the range and tidal corrections that to my experience is not justified. I strongly

suggest to estimate freeboard orbit-wise, which also gives a better handle to identify sea surface height estimation issues.

Thank you for the suggestion. We have modified our freeboard computation process slightly. However, a true on-orbit calculation produced artifacts in the data (specifically in the Ross sea) and therefore we elected not to use this method. Instead, we computed a monthly mean sea surface height grid and used on-orbit surface elevations to find freeboard. We take each surface elevation point (on-orbit) and subtract the corresponding sea surface height value to provide a measure of freeboard for each data point. This provided a better option for filtering incorrect retrievals. The remaining freeboard values are then gridded on a 25km grid. While a true on-orbit calculation would indeed be better, we feel this method is sufficient for demonstrating the retrieval results at this time.

P9L29: The description is a bit confusing, as the earlier sentences reads as snow freeboard (per grid cell) = mean elevation (per grid cell) - mean ssh (per grid cell). From this sentence I get the impression that the authors compute a mean sea surface height, remove that from the all elevations, filter anomalous elevations and then compute the snow freeboard from the remaining values. Please revise.

Agreed. This paragraph has been updated to reflect the new freeboard calculation technique.

P9L30: The authors seem to filter negative freeboards within a grid box. I assume this are then from individual waveforms? The filter should be lower than 0 meter or else the negative part of the range noise distribution will be filtered out for thinner ice and thus cause the freeboard to be biased high. In the ESA CCI dataset, the filter range for CryoSat-2 along-track freeboard is -0.25 to 2.25 meters.

Thanks for the comment. We have expanded the filter range to include negative freeboards, but have chosen a range of -0.1m to 2.1m, which has been included in the text in section 6.1.

P9L34: Is the 125km filter applied to reduce noise, or to interpolate between gaps?

Mainly, the filter is applied to reduce noise, but it also interpolates between gaps caused by filtered/missing data. The sentence "Smoothing is applied to reduce noise in the CryoSat-2 data and also to fill gaps in the data" has been added to the manuscript, section 6.1.

P10L6: The impact of surfaces waves into the ice pack also needs to be considered for CryoSat-2 data.

Thank you for pointing this out – the effects of surface waves has been included in the manuscript, as well as some possibilities for seeing high freeboard here (like lower CS-2 data density, and differing ice types found in the Antarctic MIZ). This can be found in section 6.1, paragraph 2.

P10L17ff: For this comparison it would be helpful to have corresponding maps of surface type (lead/ice) detection rates as well as average resnorm values to look into these differences and verify that the sub steps of the CryoSat-2 snow freeboard algorithm are working as intended.

This has been added to figure 5 in the manuscript (see above).

P10L16: Is the ICESat data also filtered to an effective resolution of 125 km?
That is correct – the ICESat data are filtered using the same method.

P10L26ff: It is good that the authors looked into the other output parameters of the waveform fitting. Unfortunately in this shorted form, more question are raised than answered. In essence, the retracking is based on a backscatter model of snow that when applied to CryoSat-2 waveforms, does not result in realistic snow conditions. Again, additional information such as regional differences in surface type detection rates or waveform fit quality parameters would greatly help to identify potential issues.
Verification of waveform fit quality and surface type detection has been included in the manuscript, figure 5. That said, it is not certain (at least from these figures) what is causing the unrealistic snow conditions. In the East Antarctic sector, where the "snow depth" was largest, there appears to be a larger fraction of floe-type waveforms. However, it is not anomalously large (and no larger than what is viewed in the Weddell Sea, and even smaller than the MIZ). There is an interesting region of invalid waveforms in the area, but it is small compared to the "snow depth" distribution found here, and not present elsewhere where the "snow depth" is large (such as further up the coast away from the Ross Sea). Likely, the snow-ice interface is not being tracked well, and instead found to be between 10-15 cm below the air-snow interface everywhere except the East Antarctic sector. More work will have to go into assessing the snow-ice interface elevation in future study.

P11L34: This is an overstatement given that all existing studies that used CryoSat-2 for Antarctic sea ice are not referenced in this paper.
This statement was included with intent to show the novelty of retrieving snow freeboard from CryoSat-2, though you are correct that more studies need to be referenced. We have included references to more studies throughout the paper, including in the revised introduction and here in the conclusion. This particular statement has been revised to better reflect the current state of the literature, referencing the CryoSat-2 work done by Schwegmann et al. (2016) and Paul et al. (2018), found in section 8.

P19Fig6: axis annotations and ticks are difficult to read on a printed version
This figure has been remade and should be easier to view in printed form – thank you.

Retrieval of snow freeboard of Antarctic sea ice using waveform fitting of CryoSat-2 returns

Steven W. Fons[1,2,3] and Nathan T. Kurtz[3]

[1]Department of Atmospheric and Oceanic Sciences, University of Maryland, College Park, Maryland, USA
[2]Earth System Science Interdisciplinary Center (ESSIC), University of Maryland, College Park, Maryland, USA
[3]Cryospheric Sciences Laboratory, NASA Goddard Space Flight Center, Greenbelt, Maryland, USA

Correspondence to: Steven W. Fons (steven.w.fons@nasa.gov)

Abstract In this paper we develop a CryoSat-2 algorithm to retrieve the surface elevation of the air-snow interface over Antarctic sea ice. This algorithm utilizes a two-layer physical model that accounts for scattering from a snow layer atop sea ice as well as scattering from below the snow surface. The model produces waveforms that are fit to CryoSat-2 level 1B data through a bounded trust region least squares fitting process. These fit waveforms are then used to track the air-snow interface and retrieve the surface elevation at each point along the CryoSat-2 ground track, from which the snow freeboard is computed. To validate this algorithm, we compare retrieved surface elevation measurements and snow surface radar return power levels with those from Operation IceBridge, which flew along a contemporaneous CryoSat-2 orbit in October 2011 and November 2012. Average elevation differences (standard deviations) along the flight lines (IceBridge Airborne Topographic Mapper (ATM) – CryoSat-2) are found to be 0.016 cm (29.24 cm) in 2011 and 2.58 cm (26.65 cm) in 2012. The spatial distribution of monthly average pan-Antarctic snow freeboard found using this method is similar to what was observed from NASA's Ice, Cloud, and land Elevation Satellite (ICESat), where the difference (standard deviation) between October 2011-2017 CryoSat-2 mean snow freeboard and spring 2003-2007 mean freeboard from ICESat is 1.92 cm (9.23 cm). Our results suggest that this physical model and waveform fitting method can be used to retrieve snow freeboard from CryoSat-2, allowing for the potential to join laser and radar altimetry data records in the Antarctic. Snow-ice interface elevation retrieval is also explored as a potential to obtain snow depth measurements. However, it is found that this retrieval method often tracks a strong scattering layer within the snow layer instead of the actual snow-ice interface, leading to an overestimation of ice freeboard and an underestimation of snow depth in much of the Southern Ocean but with promising results in areas such as the East Antarctic sector.

1 Introduction

Antarctic sea ice plays a complex yet important role in the earth system processes of the Southern Hemisphere. As the ice extent grows and shrinks over the course of a year, it can influence atmospheric circulations and temperatures (Cavalieri and Parkinson, 1981; Comiso et al., 2017), modify vertical and horizontal salinity profiles in the southern ocean (Aagaard and Carmack, 1989; Haumann et al., 2016), and even affect the biota of the lower latitudes (Garrison, 1991; Legendre et al., 1992; Meiners et al., 2017). Perhaps most notably, the high albedo of snow-covered Antarctic sea ice means it reflects roughly 80 % of the incoming solar radiation back to space (Allison et al., 1993; Massom et al. 2001; Brandt et al., 2005; Zatko and Warren, 2015), helping to regulate the temperature of the south polar region and balance the earth's energy budget. Unlike the Arctic Ocean, the Southern Ocean is unbounded by continents, resulting in geographically unlimited sea ice growth and vast areal extent. The average maximum extent of Antarctic sea ice is about 18.5 million km^2, occurring in September each year (Parkinson and Cavalieri, 2012). Despite a loss of sea ice extent in the Arctic since the late 1970's (Cavalieri and Parkinson, 2012), passive satellite remote sensing records of Antarctic sea ice have shown a slight increase in areal extent over the same period at a rate of about 17,100 km^2 yr^{-1} (Parkinson and Cavalieri, 2012). Over the past few

years, passive satellite observations have shown considerable variability in Antarctic sea ice extent. A record maximum extent of 19.58 million km^2 was reached on 30 September 2013 (Reid et al., 2015), only to be topped in September 2014 when the extent reached 20.11 million km^2 (Comiso et al., 2017). Less than three years later, in March 2017, sea ice cover in the Antarctic dropped to just 2 million km^2, a record low in the satellite era (Turner and Comiso, 2017). This minimum followed an unparalleled retreat of Antarctic sea ice cover in 2016 (Turner et al., 2017).

In addition to ice extent, sea ice thickness is important for gauging the state of sea ice in the polar regions. Beginning in the mid-to-late 20th century, ship-based in situ measurements provided the only thickness data available in the Southern Ocean (Worby et al., 2008). More recently, satellite altimetry instruments and techniques have proven valuable in collecting sea ice thickness information. In order to calculate thickness from altimetry, the freeboard must first be computed. Freeboard is defined as either the height of the air-snow interface above the sea surface, termed the "snow freeboard" or "total freeboard", or as the height of the snow-ice interface above the sea surface, known as the "ice freeboard". Both types of freeboard can be used to compute thickness. Typically, altimeter-based sea ice thickness is derived by assuming a hydrostatic balance and combining the freeboard measurements with a measure of the snow depth atop sea ice as well as approximations for the densities of the snow, sea ice, and sea water. In the Antarctic, snow freeboard is used most often in this calculation (Li et al., 2018), which is usually obtained using measurements from a laser altimeter.

Zwally et al. (2008) made the first estimates of satellite laser altimeter-based Antarctic sea ice thickness by utilizing data from NASA's Ice, Cloud, and Land Elevation Satellite (ICESat) taken over the Weddell Sea. They computed the snow freeboard and combined it with snow depth data taken from the Advanced Microwave Scanning Radiometer for Earth Observing System (AMSR-E). After Zwally et al. (2008), several studies retrieved pan-Antarctic sea ice thickness from ICESat, each using slightly different methods. Kurtz and Markus (2012) combined ICESat freeboards with in situ density measurements and made the "zero ice freeboard" assumption that the snow depth was equal to the snow freeboard, and thus no independent snow depth measurements were required. Kern et al. (2016) compared multiple methods of computing thickness using ICESat freeboard data, by calculating snow depths from both AMSR-E and a static but seasonally-varying snow depth to thickness ratio. A new one-layer method was developed by Li et al. (2018) to compute thickness using ICESat data that built on the static ratio used by Kern et al. (2016) and incorporated a dynamic snow depth to thickness ratio for every data point. As these studies show, a large limitation to calculating Antarctic sea ice thickness from laser altimetry, regardless of the method used, is the uncertainty in the snow depth distribution on sea ice.

In addition to using laser altimetry to calculate sea ice thickness in the Antarctic, radar altimetry has also been used in recent years. Most radar altimeters operate in the Ku band at around 13.6 GHz, a frequency that has been shown to produce a dominant backscatter from the snow-ice interface (Beaven et al., 1995). The retrieved freeboard from radar altimetry, therefore, is generally assumed to be the ice freeboard especially when the snow is relatively dry and thin. Ku-band retrievals of ice freeboard have been employed in the Arctic (Laxon et al., 2003; Laxon et al. 2013; Giles et al., 2008), where the thinner and drier snow conditions tend to exist (Webster et al., 2018). In the Antarctic, radar freeboard calculations (and subsequent thickness calculations) are complicated substantially by the depth and variable vertical structure of the snow on top of the sea ice (Willatt et al. 2010; Price et al., 2015; Kwok, 2014). Due to the wealth of available moisture from the surrounding ocean, Antarctic sea ice experiences more frequent precipitation – and therefore greater snow depths – than that of the Arctic (Massom et al., 2001; Maksym et al., 2012). The deep snow can be heavy enough to depress the sea ice surface down near or even below the sea surface, leading to flooding and wicking of the seawater within the snowpack (Massom et al., 2001; Willatt et al., 2010) that can act to obscure returns from radar altimeters. Additionally, dense, warm and/or moist snow can cause the dominant scattering surface to be located within the snowpack at a level that is higher than snow-ice interface (Giles et al., 2008; Willatt et al., 2010; Willatt et al., 2011).

2

Freeboard retrievals that neglect corrections for radar propagation through a snow layer, and thus likely track a scattering horizon at a level that is higher than the snow-ice interface, are referred to as "radar freeboards". Radar freeboard was calculated in the Antarctic by Schwegmann et al. (2016), who used data from CryoSat-2 and Envisat to retrieve freeboard with the eventual aim to create a joined Envisat-CryoSat-2 sea ice thickness record. To counteract the effects of snow scattering, Paul et al. (2018) included a snow layer range correction to radar freeboards computed using CryoSat-2 and Envisat to retrieve ice freeboard over both Arctic and Antarctic sea ice. While the method put forth by Paul et al. (2018) demonstrates usefulness in reconciling thickness between Envisat and CryoSat-2, there still exist uncertainties in the sea ice thickness retrievals brought on by the validity of the snow depth climatology used in the corrections.

When using Ku-band altimetry for retrievals of freeboard and thickness, the largest source of uncertainty comes from the snow on sea ice. Uncertainty in the depth, salinity, and vertical structure can impact ranging and freeboard calculation (Armitage and Ridout, 2015; Ricker et al. 2015; Nandan et al. 2017). In order to counteract this uncertainty and improve the knowledge of the scattering effects of a snow layer on sea ice, our work aims to utilize Ku-band altimetry from CryoSat-2 to retrieve the elevation of the air-snow interface and subsequently the snow freeboard. While it is true that Ku-band radar pulses generally penetrate the snow surface on sea ice and have a dominant scattering layer beneath, what is often not included in freeboard retrieval algorithms, especially those depending on an empirical waveform evaluation, is the fact that there are physical and dielectric differences between air and snow (Hallikainen and Winebrenner, 1992; Stiles and Ulaby, 1980) that results in scattering – albeit comparatively weaker – from the air-snow interface (discussed in Sect. 3). Though this scattering is not typically the dominant return from radar pulses, it has been shown that it can be detected from airborne as well as ground-based sensors (Kurtz et al., 2013; Willatt et al., 2010). Satellite radar returns of the air-snow interface elevation would be important in the Antarctic where snow-ice interface returns are complex and uncertain, and provide the possibility for snow depth estimations from radar altimetry. Knowledge of the snow depth in the Antarctic would enable more accurate sea ice thickness calculations, given that recent studies of Antarctic sea ice thickness rely on passive microwave snow depth data (Kern et al., 2016), assumptions of snow depth being equal to snow freeboard (Kurtz and Markus, 2012), parameterizations of snow depth from both snow freeboard (Li et al., 2018) and multi-year ice fraction (Hendricks et al., 2018), or even treatment of the snow and ice layers as a single layer with a modified density (Kern et al., 2016).

Typically, CryoSat-2 pulses are limited by the receive bandwidth (320 MHz) and therefore not able to resolve the air-snow interface explicitly (Kwok, 2014). We show that through the use of a two-layer physical model that accounts for the scattering effects of a snow layer on top of sea ice, we are able to retrack the air-snow interface from CryoSat-2 radar waveforms, compute the surface elevation, and calculate snow freeboard. Our two-layer model builds on the single-layer method developed in Kurtz et al. (2014). This study begins by explaining the datasets that are used (Sect. 2), discusses the physical rationale (Sect. 3) and method (Sect. 4) of retrieving snow freeboard from CryoSat-2, and shows an initial validation of the approach (Sect. 5). Then, the freeboard calculation, results, and comparisons are discussed in Sect. 6. Finally, a discussion on the application to snow depth retrievals and possibility for future work is provided in Sect. 7 and Sect. 8.

Antarctic sea ice plays a complex yet important role in the earth system processes of the Southern Hemisphere. As the ice extent grows and shrinks over the course of a year, it can influence atmospheric circulations and temperatures (Cavalieri and Parkinson, 1981; Comiso et al., 2017), modify vertical and horizontal salinity profiles in the southern ocean (Aagaard and Carmack, 1989; Haumann et al., 2016), and even affect the biota of the lower latitudes (Garrison, 1991; Legendre et al., 1992; Meiners et al., 2017). Perhaps most notably, the high albedo of snow-covered Antarctic sea ice means it reflects roughly 80 % of the incoming solar radiation back to space (Allison et al., 1993; Massom et al. 2001; Perovich et al., 2002), helping to regulate the temperature of the south polar region and balance the earth's energy budget. Unlike the Arctic Ocean, the Southern Ocean is unbounded by continents, resulting in

geographically unlimited sea ice growth and vast areal extent. The average maximum extent of Antarctic sea ice is about 18.5 million km², occurring in September each year (Parkinson and Cavalieri, 2012). Despite a loss of sea ice extent in the Arctic since the late 1970's (Cavalieri and Parkinson, 2012), passive satellite remote sensing records of Antarctic sea ice have shown a slight increase in areal extent over the same period at a rate of about 17,100 km² yr⁻¹ (Parkinsan and Cavalieri, 2012). Over the past few years, passive satellite observations have shown considerable variability in Antarctic sea ice extent. A record maximum extent of 19.58 million km² was reached on 30 September 2013 (Reid et al., 2015), only to be topped in September 2014 when the extent reached 20.11 million km² (Beitler, 2014). Less than three years later, in March 2017, sea ice cover in the Antarctic dropped to just 2 million km², a record low in the satellite era (Turner and Comiso, 2017). This minimum followed an unparalleled retreat of Antarctic sea ice cover in 2016 (Turner et al., 2017).

In addition to ice extent, sea ice thickness is important for gauging the state of sea ice in the polar regions. Beginning in the mid-to-late 20th century, ship-based in situ measurements provided the only thickness data available (Worby et al., 2008). More recently, active remove sensing instruments and techniques have proven valuable in collecting sea ice thickness information. Kwok et at. (2009) used NASA's Ice Cloud and land Elevation Satellite (ICESat) laser altimeter to estimate trends in sea ice thickness over the Arctic during the five year period from 2003-2008. They found that a thinning of about 0.6m occurred in multi-year ice over four years. In the Antarctic, Kurtz and Markus (2012) also utilized ICESat data to observe sea ice thickness and volume, and found that only small changes in thickness of less than -0.03 m yr⁻¹ occurred over the time period – a drastic difference from the substantial losses seen in the Arctic. Though no observations of decadal trends in Antarctic sea ice thickness currently exist, modelling studies have shown a slight increase of around 1.5 mm yr⁻¹ between 1992 and 2010 (Holland et al., 2014).

Sea ice thickness measurements from active platforms, such as those made in Kwok et al. (2009) and Kurtz and Markus (2012), are computed by first calculating freeboard from laser and/or radar altimetry. Laser altimeters operate in the visible to near infrared portion of the electromagnetic spectrum, where the emitted wavelength of the laser pulse is small enough that it scatters off of the air-snow interface and returns to the sensor with little to no penetration into the snow layer or the sea ice. Therefore, the freeboard computed from laser altimeters is the height of the air-snow interface above the sea surface, known as the "snow freeboard" or "total freeboard". Both Kwok et al. (2009) and Kurtz and Markus (2012) combine knowledge of the snow freeboard with density assumptions of ice, snow, and water, and when assuming a hydrostatic balance, compute thickness of the sea ice.

Radar altimetry is also used to estimate sea ice thickness in the polar regions. In 2003, Laxon et al. utilized data taken from radar altimeters aboard the ERS-1 and ERS-2 satellites to obtain the first estimates of satellite-derived ice thickness over the Arctic. Laxon et al. (2013) applied a similar technique using data from ESA's CryoSat-2 satellite and estimated Arctic winter sea ice thickness and volume from 2010-2012. The difference between laser and radar altimeters, however, is that most radar altimeters operate in the Ku band at around 13.6 GHz, a much longer wavelength than that of a laser altimeter. This longer wavelength allows radar pulses to penetrate the snow surface and reflect off of a layer within the snow covered sea ice, usually assumed to be the snow ice interface (Beaven et al., 1995). The freeboard computed from radar altimetry is therefore the height of the snow ice interface above the sea surface, known the "ice freeboard", and is used to calculate sea ice thickness. Radar altimeter derived ice thickness, much like that from a laser altimeter, comes from first computing sea ice freeboard and then applying the appropriate assumptions. The difference between laser and radar altimeters, however, is that most radar altimeters operate in the Ku band at around 13.6 GHz, a much longer wavelength than that of a laser altimeter. This longer wavelength allows radar pulses to penetrate the snow surface and reflect off of a layer within the snow-covered sea ice, usually assumed to be the snow-ice interface (Beaven et al., 1995). The freeboard computed from radar altimetry is therefore the height of the snow-ice interface above the sea surface, known the "ice freeboard", and is used to

calculate sea ice thickness. It is clear that for both laser and radar altimeters, accurate freeboard measurements are required in order to obtain accurate thickness measurements.

In the Antarctic, freeboard calculations are complicated substantially by the depth of the snow on top of the sea ice. Due to the wealth of available moisture from the surrounding ocean, Antarctic sea ice experiences more precipitation – and therefore greater

5   snow depths – than that of the Arctic (Massom et al., 2001; Maksym et al., 2012). The deep snow can be heavy enough to depress the sea ice down near the sea surface, leading to flooding and wicking of the seawater within the snowpack (Massom et al., 2001; Willatt et al., 2010) that can act to obscure returns from radar altimeters. Additionally, dense, warm and/or moist snow can cause the dominant scattering surface to be located within the snowpack at a level that is higher than snow-ice interface (Giles et al., 2008; Willatt et al., 2010; Willatt et al., 2011). Therefore, the assumption that scattering originates from the snow-ice interface itself can result in an

10   overestimation of the ice freeboard and in turn, the ice thickness. While it is true that Ku-band radar pulses generally penetrate the snow surface on sea ice and reflect off of a layer beneath, what is often ignored is the fact that there are physical and dielectric differences between air and snow (Hallikainen and Winebrenner, 1992; Stiles and Ulaby, 1980) that results in scattering – albeit comparatively weaker – from the air-snow interface. Though this scattering is not typically the dominant return from radar pulses, it has been shown that it can be detected from airborne as well as ground based sensors (Kurtz et al., 2013; Willatt et al., 2010).

15   Knowledge of the air-snow interface elevation can be important in the Antarctic where snow-ice interface returns are complex and uncertain.

The focus of this work is to develop a technique that retrieves the air-snow interface elevation of Antarctic sea ice from Cryosat-2 data. Typically, CryoSat-2 pulses are limited by the receive bandwidth (320 MHz) and therefore not able to resolve the air-snow interface explicitly (Kwok, 2014). We show that through the use of a two-layer physical model that accounts for the scattering

20   effects of a snow layer on top of sea ice, we are able to retrack the air-snow interface from Cryosat-2 radar waveforms, compute the surface elevation, and calculate snow freeboard. Our two-layer model builds off the single-layer method developed in Kurtz et al. (2014). This study begins by explaining the datasets that are used (Sect. 2), discusses the physical rationale (Sect. 3) and method (Sect. 4) of retrieving snow freeboard from Cryosat-2, and shows an initial validation of the approach (Sect. 5). Then, the freeboard calculation, results, and comparisons are discussed in Sect. 6. Finally, a discussion on the application to snow depth retrievals and

25   possibility for future work is provided in Sect. 7 and Sect. 8.

2 Data sets

Data for this study primarily come from ESA's Cryosat CryoSat-2 satellite, launched in 2010. The principle payload aboard CryoSat-2 is SIRAL, a Synthetic Aperture Interferometric Radar Altimeter, which has a frequency in the Ku-band at 13.575 GHz and a receive bandwidth of 320 MHz (Wingham et al., 2006). SIRAL operates in one of three modes: "low resolution" mode (LRM), "synthetic

30   aperture" (SAR) mode, and "synthetic aperture interferometric" (SARin) mode. In the Southern Hemisphere, LRM is used over the Antarctic continent and areas of open ocean and therefore is not considered in this study (Wingham et al., 2006). SAR and SARin data, which are taken over the sea ice zone and the Antarctic coastal regions, respectively, are both utilized in this work. Specifically, level 1B data from both of these operating modes are used. SAR level 1B data consist of 256 (originally 128) samples per echo while SARin data contain 512 samples per echo (Wingham et al., 2006). In order to maintain consistency between the two modes, both SAR

35   and SARin data are here truncated to 128 samples per echo.

CryoSat-2 level 1B data utilizes "multi-looking" to provide an average echo waveform for each point along the ground track. These multi-looked echoes correspond to an approximate footprint of 380 m along track and 1.5 km across track (Wingham et al., 2006). Within the level 1B data, the one-way travel time from the center range gate to the satellite center of mass is provided. This

5

information is used to retrieve elevation above the WGS84 ellipsoid. To do so, we first multiply the one-way travel time by the speed of light in a vacuum. Then, geophysical and retracking corrections are applied following Kurtz et al. (2014). These geophysical corrections are applied by using the CryoSat-2 data products, which include the ionospheric delay, dry and wet tropospheric delay, oscillator drift, dynamic atmosphere correction (which includes the inverse barometer effect), pole tide, load tide, solid Earth tide, ocean equilibrium tide, and long period ocean tide. The retracking corrections are obtained through the waveform fitting method, discussed in Sect. 4. Adding the corrections to the raw range provides the surface elevation.

For this work, CryoSat-2 data from October 2011-2017 are utilized. October was chosen so that a substantial sea ice extent is present in each year of data and also so there is overlap with the spring ICESat campaigns, which ran roughly from October to November 2003-2009. Seven years of data allows for a longer-term average to be computed and facilitates better comparison with the ICESat spring seasonal average (Sect. 6.2).

Data from NASA's Operation IceBridge airborne campaign are used in multiple capacities throughout this study. First, IceBridge 2-8 GHz Snow Radar (Leuschen, 2014) and 13-17 GHz Ku-band radar altimeter (Leuschen et al., 2014) data are used to confirm the presence of scattering of the radar beam from the air-snow interface (Sect. 3). These data are taken from flights over the Weddell Sea on 13 October 2011 and 7 November 2012, which correspond to planned underflights of a contemporaneous CryoSat-2 orbit. This flight line is known as the "Sea Ice – Endurance" mission and is shown in Fig. 1. Second, these coincident observations are used in Section 5 for direct comparisons of elevations found between IceBridge and CryoSat-2, in order to validate this CryoSat-2 algorithm. Specifically, Airborne Topographic Mapper (ATM) elevation data (Studinger, 2014) are used and compared against that of CryoSat-2.

Sea ice freeboard data taken from ICESat between 2003-2017 (Kurtz and Markus, 2012) are used primarily as a comparative measure in this work. This product is gridded to 25 km and uses a distance weighted Gaussian function to fill gaps in the gridded data. Specifically, seasonal average freeboard values from the various ICESat campaigns are compared with CryoSat-2 monthly average freeboard data obtained using this algorithm. The austral spring ICESat freeboard dataset consists of measurements made from October and November 2003-2007 (Fig. 2). These ICESat freeboard and thickness data are publicly available online at neptune.gsfc.nasa.gov/csb/index.php?section=272.

Lastly, sea ice concentration data are used to filter out grid boxes that are largely uncovered with ice. We utilize the Comiso Bootstrap monthly average product, version 3, that provides sea ice concentration on a 25 km polar stereographic grid, and remove grid boxes with monthly average concentrations less than 50 %. This product is derived using brightness temperatures from Nimbus-7 SMMR and DMSP SSM/I-SSMIS passive microwave data (Comiso, 2017).

3 Observed Ku-band scattering of radar from Antarctic sea ice

While more recent studies have shown the effects that a snow layer can have on Ku-band ranging and freeboard retrievals (Armitage and Ridout, 2015; Ricker et al. 2015; Nandan et al. 2017), past works that utilize Ku-band altimetry for ice freeboard retrieval tend to neglect scattering that occurs from the snow surface and volume, and assume that the dominant return occurs from the snow-ice interface (Beaven et at., 1995; Laxon et al. 2013; Kurtz et al. 2014). For most cases, especially in the Arctic where the snow cover is relatively thin and dry, this assumption is generally valid (Willatt et al., 2011; Armitage and Ridout, 2015). However, the physical differences between air and snow indicate that scattering can occur from the air-snow interface as well (Hallikainen and Winebrenner, 1992). This air-snow interface scattering is the fundamental basis for measuring snow freeboard using radar altimetry. Kwok (2014) used Operation IceBridge data to find that scattering from the air-snow interface does contribute to the return at Ku-

band frequencies. To further prove this fact, we use Operation IceBridge echogram data from the Ku-band and snow radars (Fig. 3) that provide a vertical profile of the radar backscatter along the flight path displayed in Fig. 1. These echograms come from the November 2012 campaign. Comparing the lower-frequency snow radar, which is known to detect the air-snow interface, with the higher frequency Ku-band radar altimeter, one can see the difference in scattering between the snow-covered floe points and the leads in both radar profiles.

In this study, a simple "peak picking" algorithm is employed to mark the vertical locations of both the maximum backscatter and the first point that rises 10 dB above the noise level for each horizontal point along the flight line. While not explicitly extracting layers from the IceBridge data, these points are used as initial guesses of the air-snow and snow-ice interfaces into the model (Sect. 4). These initial guesses are not exactly the expected backscatter coefficients from the two layers, but instead a rough approximation from their peak powers. The peak-picked air-snow interface power is compared to that of the maximum (assumed snow-ice interface) power, as displayed in Fig. 4. This frequency distribution shows that for the 2012 IceBridge campaign over Antarctic sea ice, the difference of the air-snow interface power from the maximum power is smaller for the snow radar, with a mean of 12.94 dB, than for the Ku-band altimeter, which has a mean difference of 14.00 dB. This result is expected, as it means that the scattering power from the air-snow interface is closer in magnitude to that of the snow-ice interface in snow radar returns. However, the curves have a similar distribution and mean, indicating that the Ku-band radar return likely consists of scattering from the air-snow interface as well. Overall, a comparison of the IceBridge radars provides further evidence that scattering of Ku-band radar pulses can occur at the air-snow interface. The following sections utilize this notion to retrieve snow freeboard from CryoSat-2 returns.

4 Surface elevation retrieval methodology

In this section, we introduce a new two-layer retrieval method that expands on the single layer method employed by Kurtz et al. (2014). Following that work, this study retrieves surface elevation from CryoSat-2 data by first using a physical model to simulate return waveforms from sea ice. Then, a least-squares fitting routine is used to fit the simulated waveform to the CryoSat-2 level 1B data. Sea ice parameters, including the surface elevation, can then be computed from the fit waveform. The following section describes this process. For a more detailed derivation of the theoretical basis surrounding the physical model and waveform fitting routine, see Kurtz et al. (2014).

4.1 Physical waveform model

When assuming a uniformly backscattering surface, Kurtz et al. (2014) expressed the received radar echo, $\Psi(\tau)$, as

$$\Psi(\tau) = P_t(\tau) \otimes I(\tau) \otimes p(\tau) \tag{1}$$

where τ is the echo delay time relative to the time of scattering from the mean scattering surface and $\otimes$ represents a convolution of the compressed transmit pulse, $P_t(\tau)$, the rough surface impulse response, $I(\tau)$, and the surface height probability density function, $p(\tau)$ (Brown, 1977; Kurtz et al., 2014). The terms are defined as

$$P_t(\tau) = p_0 \text{sinc}^2(B_w \tau), \tag{2}$$

where p_0 is the peak power of the pulse and B_w is the received bandwidth,

$$p(\tau) = \frac{1}{\sqrt{2\pi}\sigma_c} exp(-\frac{1}{2}(\frac{\tau}{\sigma_c})^2), \tag{3}$$

where c is the speed of light in vacuo and $\sigma_c = \frac{2\sigma}{c}$, the standard deviation of the surface height in the time domain, and

7

$$I(\tau) = \frac{\lambda^2 G_0^2 D_0\, c\, \sigma^0(0^\circ)}{32\pi h^3 \eta} \sum_{k=-\frac{N_b-1}{2}}^{\frac{N_b-1}{2}} H\left(\tau + \frac{\eta h \xi_k^2}{c}\right) exp\left[\frac{-2\xi_k^2}{\eta^2}\left(\frac{1}{\gamma_1^2}+\frac{1}{\gamma_2^2}\right) + \frac{c\eta}{h\gamma_1^2}\left(\tau + \frac{\eta h \xi_k^2}{c}\right)\right] \int_{h\gamma_1^2}^{c\eta} d\theta\, exp\left[-4\xi_k\sqrt{\frac{c}{h\eta^3}\left(\tau + \frac{\eta h \xi_k^2}{c}\right)}\cos\theta\left(\frac{1}{\gamma_1^2}+\frac{1}{\gamma_2^2}\right) - \right.$$

$$\frac{2c\cos(2\theta)}{h\eta_2^2}\left(\tau + \frac{\eta h \xi_k^2}{c}\right)\left] \left(1 + \frac{\alpha}{h^2}\left(\left(\frac{h\xi_k}{\eta}\right) + \frac{ch}{\eta}\left(\tau + \frac{\eta h \xi_k^2}{c}\right) + 2\left(\frac{h\xi_k}{\eta}\right)\cos\theta\sqrt{\frac{ch}{\eta}\left(\tau + \frac{\eta h \xi_k^2}{c}\right)}\right)\right)^{-3/2} \left(\sum_{n=0}^{N_b}\left(0.54 - 0.46\cos\left(\frac{2\pi n}{N_b}-\pi\right)\right)\right)\cos\left(2k_0 v_s\left(n-\right.\right.$$

$$\left.\left.\frac{N_b}{2}\right)\sqrt{\frac{c\tau}{\eta h}+\xi_k^2}\cos\theta-\xi_k\right)\right)^2,$$ (4)

where the variables (average values, when applicable, following Kurtz et al. (2014)) for CryoSat-2 are as follows: λ (0.0221 m) is the center wavelength, G_0 (42 dB) is the one-way antenna gain, D_0 (30.6 dB) is the one-way gain of the synthetic beam, c (299792485 m s^{-1}) is the speed of light in vacuo, $\sigma^0(0°)$ is the nadir backscatter coefficient, h (725 km) is the satellite altitude, η (1.113) is a geometric factor, N_b (64) is the number of synthetic beams, τ is the echo delay time, ξ_k is the look angle of the synthetic beam k from nadir, H is a Heaviside step function, γ_1 (6767.6) is the elliptical antenna pattern term 1, γ_2 (664.06) is the elliptical antenna pattern term 2, α is the angular backscattering efficiency, k_0 (284.307 m^{-1}) is the carrier wave number, v_s (7435 m s^{-1}) is the satellite velocity, σ is the standard deviation of surface height, and B_w (320 MHz) is the received bandwidth.

Under the assumption that only surface scattering is present and occurs from the snow-ice interface alone (i.e. no surface scattering from the air-snow interface nor volume scattering from within the snow or ice layers), Eq. (1) is able to accurately model a received CryoSat-2 echo over the Arctic (Kurtz et al., 2014). However, due to thicker snow depths on Antarctic sea ice as compared to the Arctic, scattering effects from the snow ~~surface and volume~~layer cannot be neglected when retrieving surface elevation. Therefore, Eq. (1) is here modified to become

$$\Psi(\tau) = P_t(\tau) \otimes I(\tau) \otimes p(\tau) \otimes v(\tau)$$ (5)

where $v(\tau)$ is the scattering cross section per unit volume as a function of echo delay time (Kurtz et al., 2014). Following Arthern et al. (2001) and Kurtz et al. (2014), $v(\tau)$ is defined in terms of physical parameters including the surface backscatter coefficients of snow and ice, $\sigma^0_{surf\text{-}snow}$ and $\sigma^0_{surf\text{-}ice}$, respectively, and the integrated volume backscatter of snow and ice, $\sigma^0_{vol\text{-}snow}$ and $\sigma^0_{vol\text{-}ice}$, respectively. Together, the total backscatter can be written as

$$\sigma^0 = \sigma^0_{surf-snow} + \sigma^0_{vol-snow} + \sigma^0_{surf-ice} + \sigma^0_{vol-ice}.$$ (6)

For snow on sea ice, $v(\tau)$ becomes

$$v(\tau) = \begin{cases} 0, \tau < -\frac{2h_s}{c_{snow}} \\ \sigma^0_{surf-snow}\delta\left(\tau + \frac{2h_s}{c_{snow}}\right) + \sigma^0_{vol-snow}k_{e-snow}exp\left[-c_{snow}k_{e-snow}\left(\tau + \frac{2h_s}{c_{snow}}\right)\right], 0 < \tau \le -\frac{2h_s}{c_{snow}} \\ \sigma^0_{surf-ice}k_{t-snow}^2\, exp\left[-\frac{k_{e-snow}h_s}{2}\right]\delta(\tau) + \sigma^0_{vol-ice}k_{e-ice}exp\left[-\frac{k_{e-snow}h_s}{2} - c_{ice}k_{e-ice}\tau\right], \tau \ge 0 \end{cases},$$ (7)

which accounts for signal attenuation in the snow and ice layers and loss of power at the air-snow and snow-ice interfaces. Eq. (7) comes from Kurtz et al. (2014) and uses the form of $\tau = 0$ at the snow-ice interface. In Eq. (7),

$$\sigma^0_{vol-snow} = \frac{\sigma_{vol-snow}k_{t-snow}^2}{k_{e-snow}},$$ (~~9~~8)

$$\sigma^0_{vol-ice} = \frac{\sigma_{vol-ice}k_{t-snow}^2 k_{t-ice}^2}{k_{e-ice}}.$$ (9)

Static parameters in Eqns. (7) – (9) are given values to model a snow layer on sea ice. We assign the two-way extinction coefficients of snow, $k_{e\text{-}snow}$, and sea ice, $k_{e\text{-}ice}$, to be 0.1 m^{-1} and 5 m^{-1}, respectively, following Ulaby et al. (1986). The speed of light through snow and ice are c_{snow} and c_{ice}, respectively, where $c_{snow} = \frac{c}{n_{snow}}$ and $c_{ice} = \frac{c}{n_{ice}}$. Here, $n_{snow} = 1.281$ and $n_{ice} = 1.732$, where n_{snow} corresponds to a snow layer with a density of 320 kg m^{-3} (Tiuri et al., 1984, Ulaby et al., 1986). A density of 320 kg m^{-3} was chosen

8

as an assumption to best represent pan-Antarctic snow on sea ice following results from several in situ surveys (Massom et al., 2001; Willatt et al., 2010; Lewis et al., 2011). Finally, $k_{t\text{-snow}}$ and $k_{t\text{-ice}}$ are the transmission coefficients between the air-snow and snow-ice interfaces, respectively. Both transmission coefficients are generally close to one (Onstott, 1992); we use values of $k_{t\text{-snow}}=0.9849$ and $k_{t\text{-ice}} = 0.9775$ as calculated from the Fresnel reflection coefficient using the values of n_{snow} and n_{ice}. h_s, the snow depth, is computed from the echo delay shift of the air-snow and snow-ice interfaces, free parameters t_{snow} and t respectively, which are discussed in Sect. 4.3. The remaining free parameters are given as inputs to the model and are defined in the following section.

The main assumption in this approach is that scattering is expected to come from two defined layers (i.e. the air-snow and snow-ice interfaces) and uniformly throughout the volume. ~~Though~~ Antarctic sea ice can exhibit complex layer structures that could obscure this simple two-layer method, <u>however,</u> no pan-Antarctic understanding of snow-covered sea ice composition currently exists. Therefore, this two-layer assumption is utilized as an approximation of the broad-scale sea ice cover.

4.2 Waveform fitting routine

To fit the modelled waveform to CryoSat-2 data, a bounded trust region Newton least-squares fitting routine (MATLAB function *lsqcurvefit*) is employed. This routine fits the model to the data by iteratively adjusting model input parameters and calculating the difference between the modelled and CryoSat-2 level 1B waveform data, until a minimum solution – or the established maximum number of iterations – is reached. Building off of Kurtz et al. (2014), this process can be shown with the equations

$$P_m(\tau) = A_f L(\tau, \alpha, \sigma) \otimes p(\tau, \sigma) \otimes v\left(\tau, t_{snow}, \sigma^0_{surf-snow}, \sigma^0_{surf-ice}, \sigma^0_{vol-snow}, \sigma^0_{vol-ice}\right) \tag{10}$$

and

$$min \sum_{i=1}^{128}[P_m(\tau_i) - P_r(\tau_i + t)]^2, \tag{11}$$

where L is a lookup table of $P_t(\tau) \cdot \otimes I(\tau)$ as defined in Kurtz et al. (2014), P_m is the modelled waveform, P_r is the observed echo waveform, and τ_i is the observed echo power at point i on the waveform. These equations result in nine free parameters: the amplitude scale factor, A_f, the echo delay shift factor at the air-snow and snow-ice interfaces, respectively t_{snow} and t, the angular backscattering efficiency, α, the standard deviation of surface height, σ, and the terms that together make up the total backscatter, $\sigma^0_{surf-snow}$, $\sigma^0_{surf-ice}$, $\sigma^0_{vol-snow}$, and $\sigma^0_{vol-ice}$. These parameters are adjusted with each iteration of the fitting routine and are explained further in Sect. 4.3.1 and Sect. 4.3.2. An initial guess for each of the free parameters – in addition to upper and lower bounds – is provided to the fitting routine. Doing so ensures that the solution reached will closely resemble that of the physical system. Approaches for determining the initial guesses for both lead and floe characterized echoes are outlined in the following section.

This algorithm uses the squared norm of the residual ("resnorm") as a metric for goodness of fit. Modelled waveforms with a resnorm less than or equal to 0.3 are considered to be good fits and have the output parameters used in the retracking correction calculation and surface elevation retrieval. Waveforms with greater fitting error are run again using a different initial guess for α. If the resnorm is still high, the CryoSat-2 echo is not used in the retrieval process. <u>Figure 5 shows a spatial distribution of the mean October resnorm values for 2011-2017. The largest residuals are consistently located around the ice edge and near to the continent, while the smallest are collocated with areas of high lead-type fraction (Fig. 5), such as the Ross Sea. Since the specular lead waveforms are easily fit with little residual, the overall average distribution shown here is consistently under 0.3 (total mean of 0.13). However, many floe-type points have values closer to the 0.3 threshold. Although</u> ~~Although~~ we have observed that a resnorm threshold of 0.3 results in reasonably representative modelled waveforms, we understand that the use of a single metric can oversimplify the goodness of fit and leaves room for errors in the shape of the modelled waveform. Future work will look into a incorporating a more comprehensive metric for goodness of fit.

9

4.3 Lead / floe classification

Prior to constructing a physical model and fitting it to the data, each CryoSat-2 echo is first characterized as either a lead or a floe based on parameters derived from the individual waveform. Specifically, the pulse peakiness (PP) and stack standard deviation (SSD) parameters are used to distinguish between the two surface types, following Laxon et al. (2013). PP is defined as

$$PP = max(P_r) \sum_{i=1}^{128} \frac{1}{P_{r(i)}} \qquad (12)$$

from Armitage and Davidson (2014). SSD comes from the CryoSat-2 level 1B data product and is due to the variation in the backscatter as a function of incidence angle (Wingham et al., 2006). Figure 5 shows average detection rates for lead and floe points using this method, discussed in the following sections.

4.3.1 Leads

CryoSat-2 echoes are categorized as leads if the return waveform has a PP > 0.18 and a SSD < 4 (Laxon et al., 2013). Since by definition leads have no snow cover, it is assumed that all scattering of the radar pulse originates from one surface. In this case, that surface is either refrozen new ice or open water. It is also assumed that no volume scattering occurs from leads. Therefore, the volume scattering term in Eq. (10) goes to a delta function at $\tau = 0$, resulting in four free parameters: the amplitude scale factor, A_f, the echo delay shift factor, t, the angular backscattering efficiency, α, and the standard deviation of surface height, σ. The initial guess for A_f is set equal to the waveform peak power, with the bounds set to +/- 50 % of the peak power. The echo delay shift, t, is given an initial guess equal to the point of maximum power, denoted with t_i. σ is first estimated to be 0.01 for lead points, with bounds taken to be $0 \leq \sigma \leq 0.05$. The initial guess for α, denoted as α_0, is calculated as the ratio of tail to peak power and uses a mean of the 10ns following the location of peak power. The bounds of α are $\frac{\alpha_0}{100} \leq \alpha_0 \leq 100\alpha_0$. Using the above initial guesses in the fitting routine leads to a modelled waveform that well represents the CryoSat-2 data over leads (Kurtz et al., 2014). The echo delay factor, t, provides the location of the surface as a function of radar return time, which is used in the surface elevation retrieval of each lead-classified echo. The largest fraction of lead-classified points occurs in the Ross Sea, consistent with the location of the Ross Sea Polynya (Fig. 5). However, it is also a region known for new-ice formation that could return specular lead-type waveforms, and potentially lead to an overestimation of the sea surface height (discussed in section 6).

4.3.2 Floes

Radar echoes with a PP < 0.09 and a SSD > 4 are classified as sea ice floes (Laxon et al., 2013). Due to the presence of a snow layer on top of the sea ice, all nine free parameters (introduced in Sect. 4.2) are employed. These include the four mentioned in the previous section, as well as t_{snow}, the echo delay shift factor of the air-snow interface, $\sigma^0_{surf-snow}$, $\sigma^0_{vol-snow}$, $\sigma^0_{surf-ice}$, and $\sigma^0_{vol-ice}$. The initial guess and bounds for A_f is taken to be the same as used for lead points, while the remaining 8 differ from leads. For t_{snow}, the initial guess (t_{i-snow}) comes from the ICESat datasets of the seasonal average total freeboard ~~datasets~~. We use the "zero ice freeboard" assumption (Kurtz et al., 2012) that the snow-ice interface is depressed to the sea surface, meaning the ICESat freeboard would be approximately equal to the snow depth. Though this assumption is generally thought to be valid in the Antarctic, it may not hold true in all regions of the Antarctic (Adolphs, 1998; Weissling and Ackley, 2011; Xie et al., 2011; Kwok and Maksym, 2014). Therefore, this fitting routine attempts to adapt and move away from the zero ice freeboard assumption, with the results being explored in later sections. The ICESat freeboard height at the location of each CryoSat-2 radar pulse is taken and converted in terms of radar return time, which provides a suitable initial guess of the air-snow interface. Bounds of t_{i-snow} are taken to be +/- 5 ns. The initial guess for t

(t$_i$) is taken to be the first point where the waveform power reaches 70 % of the power of the first peak, following Laxon et al. (2013). This is a commonly used threshold retracking method to detect the snow-ice interface from CryoSat-2. Bounds are taken to be +/- 6 ns. σ is first estimated to be 0.15 for floe points, with bounds set to $0 \leq \sigma \leq 1$. The initial guess for α is similar to that in the lead characterization, with the exception that the mean power of points between 90 ns and 120 ns is used in the ratio of tail to peak power. Bounds for α$_0$ are set as $\frac{\alpha_0}{100} \leq \alpha_0 \leq 100\alpha_0$.

The remaining surface backscatter coefficients and integrated volume backscatter of snow and ice are initially estimated using values taken from Operation IceBridge Ku-band radar echograms from the Weddell Sea flights. Estimation of the surface backscatter comes from an average of all valid peaks chosen from the echogram peak-picker for the ~~respective surfaces~~air-snow and snow-ice interfaces of both flights. The snow and ice volume backscatter values are parameterized using average layer backscatter values between the two interfaces and 10 range bins beyond the snow-ice interface, respectively. The initial guesses (bounds) are set to be as follows: $\sigma^0_{surf-snow}$ = -15 dB (+/- 5 dB), $\sigma^0_{vol-snow}$ = -11 dB (+/- 5 dB), $\sigma^0_{surf-ice}$ = -1 dB (+/- 10 dB), and $\sigma^0_{vol-ice}$ = -8 dB (+/- 10 dB). The largest fraction of floe-type points are found in the Weddell Sea and along the ice edge, where older and rougher ice is generally found (Fig. 5). These distributions compare qualitatively to that found in Paul et al. (2018), with the exception that this method finds a larger region of lead-type dominant waveforms in the Ross Sea than Paul et al. (2018).~~An example CryoSat 2 floe waveform and fit is shown in Fig. 5.~~

The modelled waveform (examples shown in Fig. 6) is sensitive to the initial guess provided, and therefore care was taken to ensure the initial guesses come from physically realistic values. A change in the initial guesses results in different final fits, and subsequently a different freeboard distribution. Figure 6 shows a waveform sensitivity study looking at a variety of modeled waveforms that differ only in the initial guess for the standard deviation of surface height (σ, top) and the total backscatter coefficient (σ^0, bottom). The range of σ was taken to be between 0.01 (very smooth surface) to 0.4 (rough surface), while σ^0 was varied between three different parameterizations: values from Kurtz et al. (2014), values taken from the IceBridge Snow Radar data, and from the Ku-band data (above). The resulting freeboard distributions found using an initial guess of σ = 0.35 and σ^0 taken from Kurtz et al. (2014) are shown as a difference from the values chosen in this study (σ = 0.15, σ^0 taken from Ku-band radar data) in Fig. 6 (C and F). It is evident that physically inconsistent initial guesses can result in altered freeboard distributions. In this case, the effect of altering the backscatter parameterization had a larger effect on freeboard than altering σ. Thus, a potential future area of study will be to determine better empirical first guess choices for the static free parameters currently used in the model.

5 Initial validation

To evaluate the performance of this algorithm, the returned surface elevation is compared to independent measurements of surface elevation from Operation IceBridge. Specifically, ATM data taken from the IceBridge underflight of the CryoSat-2 orbit (Fig. 1) is compared with retracked CryoSat-2 elevation data ~~found~~ derived using this algorithm. The comparison is done between surface elevation measurements before any freeboard calculations are made, ensuring that differences observed are a factor of the retrieval alone. In order to facilitate a direct comparison, ATM level 2 Icessn elevation data are averaged to the same ground footprint size as a CryoSat-2 echo. Additionally, equivalent geophysical corrections are computed and applied (following ~~Kurtz et al., 2013~~Yi et al., 2018) to both the CryoSat-2 and ATM datasets, ensuring that both measurements are in the same frame of reference. These geophysical corrections include effects from tides, which are computed using the TPXO8-Atlas model (Egbert and Erofeeva, 2002), the mean sea-surface height, which are computed using the Technical University of Denmark DTU15MSS dataset (Anderson et al., 2016), and the dynamic atmosphere, which are computed using correction data from the Mog2G model (Carrère and Lyard, 2003).

Surface temperatures from MERRA-2 (GMAO, 2015) at the midpoint time of both IceBridge flights are found in Fig. 1. The 2011 flight had a large (about 20 °C) north-south temperature gradient that could result in different snow and ice properties along the flight line, and thus could explain differences observed along the line. In 2012, there was almost no temperature gradient along the flight line. According to the EUMETSAT OSI SAF sea ice type product (www.osi-saf.org), both flights were sampling above first year ice for the entirety of the campaigns. Additionally, surface temperatures remained below freezing for the two weeks prior to both flights, with light snowfall of around 5 mm day^{-1} occurring three (four) days prior to the flight in 2011 (2012) but stopping two (three) days before the flight. The time difference between the IceBridge flight and CryoSat-2 overpass was between 0 and 3.1 hours in 2011 and between 0 and 2.2 hours in 2012.

~~Figure 6~~Figure 7 (A and B) shows ATM and CryoSat-2 surface elevation profiles from both the 2011 and 2012 IceBridge underflights. In these cases, the initial guess for the air-snow interface location in the CryoSat-2 fitting routine comes from the ICESat seasonal average dataset. Overall, the CryoSat-2 retracked elevation profiles capture the general trends found in the ATM profiles. ~~Both datasets appear to detect similar locations of troughs and ridges along the flight line, with some discrepancy in the magnitude of each.~~ The mean difference in elevation of CryoSat-2 from ATM for the entire flight line is 0.016 cm in 2011 and 2.58 cm in 2012. A frequency distribution of this difference is shown in ~~Fig. 6~~Fig. 7 (C and D). Both years display a Gaussian-like distribution centered near zero (i.e. no difference) with standard deviations of 0.29 m in 2011 and 0.27 m in 2012. It is likely that some of the differences are due to initial temporal and spatial discrepancies between the IceBridge and CryoSat-2 data collections. Correlations coefficients are 0.44 in 2011 and 0.40 in 2012, which, although in the low-to-mid range, is likely brought on by the inherent noise in the data at the shot-to-shot level and non-overlapping footprints of the two sensors (Yi et al., 2018). Although mean resnorm values from the CryoSat-2 flight lines are 0.1124 in 2011 and 0.0990 in 2012, signifying good fits, it is still possible that errors in air-snow interface elevation could have arisen from errors in fits that were below the single-metric resnorm threshold but not representative of the actual CryoSat-2 waveform. This resnorm threshold is likely the cause of the "jumps" seen in the CryoSat-2 data, as testing a higher resnorm threshold led to more jumps, while a testing a lower resnorm threshold led to fewer jumps, but worse agreement to ATM. There also appears to be a slight underestimation of ATM by CryoSat-2 in both profiles, which could be brought on by the original footprint sizes, as the smaller ATM footprint is more sensitive to small-scale peaks/ridges than CryoSat-2.

Overall, this initial validation shows the potential of our CryoSat-2 algorithm to retrieve reasonable surface elevation measurements over Antarctic sea ice. This promising result warrants further exploration into freeboard retrieval using this method, discussed in the next section.

6 Snow freeboard retrieval

6.1 Freeboard calculation

The retrieved elevation of the air-snow interface from this method is used to calculate the snow freeboard of Antarctic sea ice. First, one month of CryoSat-2 data is processed at a time and the outlying data points are filtered out to reduce the inherent noise of the data. The filtering is done by removing any point that has an output parameter more than three standard deviations away from the mean of the respective parameter. These output parameters include quantities such as the surface elevation, retracking correction, PP, SSD, and τ. Additionally, points with a τ value less than -100 ns were found to produce anomalous surface elevations and therefore are filtered out. Then, surface elevation dat~~The surface elevation data are then gridded to a 25 km polar stereographic grid and averaged over the month, resulting in a single grid of air-snow interface elevation values. Grid boxes are ignored if they contain fewer than five data points or have a monthly average sea ice concentration of less than 50 %. a~~A consisting only of echo points characterized as leads

are gridded to a new 25 km polar stereographic grid is created consisting only of echo points characterized as leads, and is also averaged over the month. Once again, gGrid boxes with fewer than five points and/or monthly concentrations less than 50 % are ignored. This second grid is effectively the mean sea surface elevation. Finally, Ssnow freeboard is calculated by subtracting taking each surface elevation point along the CryoSat-2 orbit and subtracting the corresponding the mean sea surface elevation grid value. from the air-snow interface elevation grid. Anyy points within each grid box with a negative or anomalous (greater than 2 m) snow freeboard points less than -0.1m and greater than 2.1m are filtered out and are no longer included in the average of the grid box. Between the initial filtering and this freeboard filtering, 41.68% of the total waveforms are filtered out, leaving 58.32% as valid waveforms. This process is done from the entire month of data, and the remaining freeboard values are gridded to 25 km to produce a map of the monthly mean snow freeboard. To study multi-year means for a given month, each monthly snow freeboard grid is averaged over a range of years. In this case, grid boxes with data from fewer than two years are ignored. Both the monthly and multi-year mean snow freeboard grids are smoothed by taking the average of all grid boxes within 2 grid boxes in all directions, which reduces the spatial resolution to 125 km. Smoothing is applied to reduce noise in the CryoSat-2 data and also to fill gaps in the data.

Figure 7Figure 8 shows maps of October monthly averaged snow freeboard values from 2011-2017 as well as the mean of all seven years. The freeboard distribution corresponds well to what is expected in the Antarctic: the largest values occur in the Weddell and Amundsen seas – where ice production and heavy snow falls are typically prevalent – as well as along the coast of East Antarctica – where snowfall accumulation is also typically large. The smallest values tend to be found off the coast of East Antarctica between 0° and 90° E. Additionally, the region of low freeboard shown in the Ross Sea each year is consistent with the presence of young ice from the Ross Sea Polynya, but could be biased lower due to the large region of lead-type waveforms classified in the area, leading to a higher sea surface height and lower freeboard. While the overall pattern remains similar in each map, there is clear inter-annual variability. For example, the Amundsen Sea region along the Antarctic coastline exhibits a widespread area of very large (over 50 cm) freeboard in 2011, while the same coastal region between 100° W and 150° W shows values between 20 and 35 cm in 2016. Thicker snow freeboard can be found adjacent to the ice extent edge in each of the years, with the average map clearly showing greater freeboard values along the ice edge in the Western Pacific Ocean (about 90° E to 180° E). This thick freeboard at the ice edge is consistent with the older and thicker ice that has been previously found in the Antarctic frontal ice zone (Nghiem et al., 2016), but could also be due to surface waves penetrating the ice cover, resulting in an altered floe size distribution (Fox and Haskell, 2001) and also a high freeboard bias. Additionally, the high freeboard found here could be a product of the lower CryoSat-2 data density further from the pole as well as the variety of different ice types found in the frontal ice zone.

A time series of mean October snow freeboard from 2011 to 2017 found using this method is shown in Fig. 8Fig. 9, with total sea ice area plotted for reference (Fetterer et al., 2017). Apart from slight increases in freeboard from 2012 to 2013 and 2016 to 2017, there is an overall decrease found between 2011 and 2017 of 0.5θ cm yr^{-1}. The smallest measured freeboard occurred in 2016 (25.77 8 cm) which is collocated with a minimum in sea ice area that occurred in the same year. The total average snow freeboard in October from 2011 to 2017 is found to be 27.6 cm with a standard deviation of 12.97 3.0 cm. Interestingly, the sea ice area and snow freeboard time series appear highly correlated between 2011 and 2017 (r=0.779001) alluding to a potential relationship between freeboard/thickness and area in the Antarctic. This relationship, however, is beyond the scope of this paper and will be explored in future work.

6.2 Comparison Pan-Antarctic freeboardto comparisonsICESat

To assess the performance of this algorithm on a pan-Antarctic scale, monthly averaged freeboard values from CryoSat-2 are compared with seasonal average freeboard from ICESat. Figure 9Figure 10 shows a difference map between CryoSat-2 and ICESat total

13

freeboard, where positive (negative) values indicate regions where CryoSat-2 measures greater (smaller) freeboard as compared to ICESat. The most notable difference occurs in the Weddell Sea off of the Antarctic Peninsula, where CryoSat-2 records a freeboard value much lower (around 30 cm) than ICESat. A similar region can be found in the Amundsen Sea, where CryoSat-2 measurements are again less than ICESat. CryoSat-2 measures a larger freeboard along most of the sea ice edge, as well as along the Antarctic coast from about 20° W to 60° E. Apart from these areas of noticeable differences between the two data sets, the remainder of the sea ice zone is fairly comparable among both. The total mean difference is only 2~~1~~.9 cm with a standard deviation of just ~~over~~ under 10 cm and a mode difference of 0.8 cm (~~Fig. 9~~Fig. 10).

Th~~ough this~~is compatibility is encouraging, it is important to note that ~~considering that the~~ comparison is ~~only seasonal and not directly month-to-month.~~indirect in nature. The CryoSat-2 dataset covers October 2011-2017, seven years of data, while this ICESat dataset covers October-November 2003-2007, five years of data. These non-overlapping time periods have different lengths, and the ICESat dataset contains data from October and November in some of the campaigns. Therefore, this comparison shows that our algorithm can produce results similar to the average values found with ICESat, but requires temporally coincident data, such as that forthcoming from ICESat-2, to best assess the accuracy of the retrieval approach.

Qualitatively, the snow freeboard distribution found in Fig. 8 is comparable to that shown in Schwegmann et al. (2016) and Paul et al. (2018). In all studies, the largest freeboard is found along the coast in the Amundsen Sea, East Antarctica, and in the Weddell Sea, while the smallest freeboard is found in the Ross Sea and off East Antarctic between 0° and 90° E. Similar to what was found in the comparison with ICESat, both Schwegmann et al. (2016) and Paul et al. (2018) find a higher freeboard immediately off the Antarctic Peninsula near the Larson Ice Shelf than is found with this method, which could signal a regional difficulty to retrieve snow freeboard using this algorithm or a complication with the thicker and/or rougher ice that tends to be found in this region. However, these comparisons are still rather indirect, given that the prior works retrieve radar freeboard (Schwegmann et al., 2016) and ice freeboard (Paul et al., 2018) while this method retrieves snow freeboard. Once again, coincident measurements of snow freeboard from ICESat-2 will be invaluable as a comparative tool.

7 Application to snow depth retrievals

Given that this algorithm outputs the location of both the air-snow and snow-ice interfaces as a function of radar return time, it seems logical that snow depth could be extracted from these data. Likely, however, the complexities of Antarctic sea ice inhibit this method in tracking the correct snow-ice interface, resulting in a lower-than-expected (judging from passive microwave measurements (Markus and Cavalieri, 1998) and in-situ surveys (Massom et al., 2001)) snow depth distribution~~.~~ ~~Figure 10~~Figure 11 shows a map of the average October 2011-2017 snow depth on sea ice, calculated by subtracting the snow-ice interface elevation from the air-snow interface elevation. It can be seen that for a majority of the Antarctic, a snow depth of around 0.1 m is present. This algorithm appears to be tracking the ~~snow-ice interface~~dominant sub-surface return as a layer within the snowpack as opposed to the ice interface itself, as has been seen in previous studies (e.g. Giles et al., 2008; Willatt et al., 2010). A potential explanation is that the complex snow stratigraphy found during in situ surveys of the Antarctic sea ice pack (Massom et al., 2001; Willatt et al., 2010; Lewis et al., 2011) and attenuation due to seawater flooding and wicking could be prevalent throughout the Antarctic, and that ~~features such as~~layers of ice ~~y layers~~ and/or ~~wicking~~ brine could be responsible for a~~n~~ ~~snow-ice~~ interface return that is higher than the actual snow-ice interface.

A similar result is found when comparing retrieved CryoSat-2 snow depths in the Weddell Sea to that from Operation IceBridge. Using the peak-picking algorithm on IceBridge data from the 13 October 2011 flight line, we calculate an approximate mean snow depth of 0.26~~4~~ m. This value is close to the snow depth that was calculated by Kwok and Maksym (2014, table 2 S2-S4) for the same flight line (approximately 0.29~~0~~ m). From CryoSat-2, the mean snow depth along the flight line is found to be 0.15~~2~~ m,

14

which is lower than the measured values potentially due to the much larger footprint size and more limited bandwidth from the satellite data.

Despite the widespread small snow depth values, the region off the coast of East Antarctica in ~~Fig. 10~~Fig. 11 (between 90° E and 60° E) exhibits values closer to what is expected. Here, there is a ~~slightly~~ greater snow depth of around 0.3 m. This region is known to have positive ice freeboard values (Worby et al., 1998; Maksym and Markus, 2008; Markus et al., 2011) meaning that flooding and saltwater intrusion would play less of a role than in other areas. The near-realistic snow depth measurements here provide evidence that our algorithm could be effective in retrieving snow depth under certain snow conditions, seasons, or locations, but speaks to the inherent complexity and uncertainty associated with Antarctic sea ice. More work is needed in ~~validating~~ evaluating the tracking of the snow-ice interface using this method to ~~better understand the~~use it together with the air-snow interface for ~~snow depth ~~distribution~~ on sea ice estimation.

8 Conclusions and future work

In this work, a method for retrieving snow freeboard from CryoSat-2 data is developed. It is based off the fundamental idea that scattering of Ku-band radar pulses can originate from the air-snow interface of snow on sea ice. We incorporate this scattering into a physical waveform model and use a least squares fitting routine to fit the model to CryoSat-2 level 1B waveforms. The returned fit waveform and associated parameters includes, among others, the location of the air-snow interface as a function of radar return time. We are able to use that location to retrack the snow surface elevation, and from this, calculate snow freeboard. Through a comparison of this method with independent measurements, we are able to ~~validate~~ evaluate the performance of our retrieval. Specifically, surface elevation measurements from Operation IceBridge ATM, taken in October 2011 and November 2012 along a coincident flight line, help to provide an initial confirmation that the retrieval results were comparable to other data sources. Mean (standard deviation) elevation differences between ATM and CryoSat-2 were found to be just 0.016 cm (29.24 cm) in 2011 and 2.6 cm (26.65 cm) in 2012. Seasonal averaged freeboard data from ICESat allowed for the comparison of the pan-Antarctic freeboard. Though the CryoSat-2 and ICESat freeboard data ~~from~~ come from non-overlapping time periods of different lengths and months~~s from October 2011-2017 while ICESat data comes from October and November 2003-2007~~, there was still general agreement with the freeboard distribution. The mean (standard deviation) difference between CryoSat-2 and ICESat freeboard is 2~~1~~.9~~42~~ cm (9.23 cm). In general, this retrieval algorithm shows promise that snow freeboard can be measured from CryoSat-2 alone.

Though the retrieved air-snow interface elevation and snow freeboard closely resembles that from independent measurements, the retrieved ~~ice freeboard~~snow-ice interface elevation appears to be larger than expected. Calculated snow depth, therefore, is lower than typically expected throughout most of the Antarctic sea ice cover as compared to in situ and passive microwave data. Due to strong attenuation of radar returns from brine layers within ~~flooded sea ice~~the snow pack (Nandan et al., 2017), it may not be possible to retrieve the actual snow-ice interface from a Ku-band altimeter in some regions of the Antarctic. However, the region near the Antarctic coast in the Western Pacific Ocean (~~Fig. 10~~Fig. 11) displays snow depths that are much closer to expected, signaling the possibility of snow depth retrieval under certain ice types and conditions.

Overall, this study has expanded the functionality of CryoSat-2 as a tool for observing the snow freeboard of Antarctic sea ice, adding to the existing studies retrieving radar freeboard (Schwegmann et al., 2016) and ice freeboard (Paul et al., 2018). In September 2018, CryoSat-2 ~~will be joined~~was joined in space by ICESat-2, NASA's second-generation satellite laser altimeter system (Markus et al., 2017). These coincident altimeters will provide the ability to observe the polar regions like never before. For this work specifically, ICESat-2 data will be used as both a comparative measure – for direct monthly comparisons of snow freeboard – as well

as an initial guess for the waveform fitting model. These new measurements of air-snow interface elevation and snow freeboard from ICESat-2 will help to further validate this retrieval algorithm.

Future work will look into combing these ~~Cryosat~~CryoSat-2 snow freeboard measurements with those from laser altimetry to produce an ICESat-CryoSat-2-ICESat-2 time series of snow freeboard in the Antarctic. This reconciled laser-radar altimetric record of snow freeboard would span 15+ years from 2003 throughout the lifetime of ICESat-2, providing a long and robust dataset that could be used in other studies of sea ice. Together with ESA's Climate Change Initiative dataset combing CryoSat-2 and Envisat (Schwegmann et al., 2016; Paul et al., 2018), these long term~~A~~ dataset~~s~~ ~~of this scale~~ could lead to improved retrievals of sea ice thickness and an enhanced understanding of ~~snow~~ sea ice ~~freeboard~~ in the Antarctic~~.~~~~, allowing for improved retrievals of Antarctic sea ice thickness.~~

9 Author contribution

N.K. developed the framework model and fitting code. S.F. adapted the code and carried out the analysis. S.F. prepared the manuscript with contributions from N.K.

10 Competing interests

The authors declare that they have no conflict of interest.

References

Aagaard, K. and Carmack, E. C.: The role of sea ice and other fresh water in the Arctic circulation, J. Geophys. Res., 94, 14485-14498, doi:10.1029/JC094iC10p14485, 1989.

Adolphs, U.: Ice thickness variability, isostatic balance and potential for snow ice formation on ice floes in the south polar Pacific Ocean, J. Geophys. Res.-Oceans, 103, 24675-24691, doi:10.1029/98JC02414, 1998.

Allison, I., Brandt, R. E., and Warren, S. G.: East Antarctic Sea Ice: Albedo, Thickness Distribution, and Snow Cover, J. Geophys. Res., 98, 12417-12429, doi:10.1029/93JC00648, 1993.

Anderson, O. B., Stenseng, L., Piccioni, G., and Knudsen, P., The DTU15MSS (Mean Sea Surface) and DTU15LAT (Lowest Astronomical Tide) reference surface, Paper presented at the ESA Living planet symposium 2016, Prague, Czech Republic. Retrieved from ftp.space.dtu.dk/pub/DTU15/DOCUMENTS/MSS/DTU15MSS+LAT.pdf, 2016.~~.~~

Armitage, T. W. K. and Davidson, M. W. J.: Using the interferometric capabilities of the ESA CryoSat-2 mission to improve the accuracy of sea ice freeboard retrievals, IEEE Trans. Geosci. Remote Sens., 52, 529–536, 2014.

Armitage, T. W. K. and Ridout, A. L.: Arctic sea ice freeboard from AltiKa and comparison with CryoSat-2 and Operation IceBridge, Geophys. Res. Lett., 42, 6724-6731, doi:10.1002/2015GL064823, 2015.

16

Arthern, R. J., Wingham, D. J., and Ridout, A. L.: Controls on ERS altimeter measurements over ice sheets: Footprint scale topography, backscatter fluctuations, and the dependence of microwave penetration depth on satellite orientation, J. Geophys. Res., 106, 33471–33484, 2001.

Beaven, S. G., Lockhart, G. L., Gogineni, S. P., Hosseinmostafa, A. R., Jezek, K., Gow, A. J., Perovich, D. K., Fung, A. K., and Tjuatja, S.: Laboratory measurements of radar backscatter from bare and snow-covered saline ice sheets, Int. J. Remote Sens., 16, 851–867, 1995.

Brandt, R. E., Warren, S. G., Worby, A. P., and Grenfell, T. C.: Surface Albedo of the Antarctic Sea Ice Zone, J. Climate, 18, 3606-3622, doi:10.1175/JCLI3489.1, 2005.

Beitler, J., 2014 melt season in review, National Snow and Ice Data Center, 2014. Accessed July 2018.

Brown, G. S.: The average impulse response of a rough surface and its applications, IEEE Trans. Antennas Propagat., AP-25, 67–74, January 1977.

Carrère, L., and Lyard, F., Modeling the barotropic response of the global ocean to atmospheric wind and pressure forcing – comparisons with observations, Geophys. Res. Lett., 30, 1275, 8, doi:10.1029/2002GL016473, 2003.

Cavalieri, D. J. and Parkinson, C. L.: Large-Scale Variations in Observed Antarctic Sea Ice Extent and Associated Atmospheric Circulation, Mon. Weather Rev., 109, 2323-2336, doi:10.1175/15200493(1981)109<2323:LSV-IOA>2.0.CO;2, 1981.

Cavalieri, D. J. and Parkinson, C. L.: Arctic sea ice variability and trends, 1979-2010, The Cryosphere, 6, 881-889, doi:10.5194/tc-6-881-2012, 2012.

Comiso, J. C.: Bootstrap Sea Ice Concentrations from Nimbus-7 SMMR and DMSP SSM/I-SSMIS, Version 3, October 2011-2017, Boulder, Colorado, USA, USA, National Snow and Ice Data Center Distributed Active Archive Center, doi:10.5067/7Q8HCCWS4I0R, 2017.

Cavalieri, D. J., Parkinson, C. L., Gloersen, P., and Zwally, H. J.: Sea ice concentrations from Nimbus-7 SMMR and DMSP SSM/I Passive Microwave Data, Version 1, October 2006-2017, Boulder, Colorado, USA, National Snow and Ice Data Center Distributed Active Archive Center, doi:10.5067/8GQ8LZQVL0VL, 1996, updated yearly.

Comiso, J. C., Gersten, R. A., Stock, L. V., Turner, J., Perez, G. J., and Cho, K.: Positive Trend in the Antarctic Sea Ice Cover and Associated Changes in Surface Temperature, J. Climate, 30, 2251-2267, doi:10.1175/JCLI-D-16-0408.1, 2017.

Egbert, G. D., and Erofeeva, S. Y., Efficient Inverse Modeling of Barotropic Ocean Tides, J. Atmos. Ocean Tech., 19, 183-204, doi:10.1175/1520-0426(2002)019<0183:EIMOBO>2.0.CO;2, 2002.

Fetterer, F., Knowles, K., Meier, W., Savoie, M., and Windnagel, A. K., Sea Ice Index, Version 3, October 2011-2017, Boulder, Colorado USA, NSIDC: National Snow and Ice Data Center, doi:10.7265/N5K072F8, 2017, updated daily.

Fox, C. and Haskell, T. G.: Ocean wave speed in the Antarctic marginal ice zone, Ann. Glaciol., 33, 350-354, doi:10.3189/172756401781818941, 2001.

Garrison, D. L.: Antarctic Sea Ice Biota, Am. Zool., 31, 17-34, doi:10.1093/icb/31.1.17, 1991.

Giles, K. A., Laxon, S. W., and Worby, A. P.: Antarctic sea ice elevation from satellite radar altimetry, The Cryosphere Geophys. Res. Lett., 35, L03503, doi:10.1029/2007GL031572, 2008.

Global Modeling and Assimilation Office (GMAO): MERRA-2 tavg1_2d_ocn_Nx: 2d,1-Hourly,Time-Averaged,Single-Level,Assimilation,Ocean Surface Diagnostics V5.12.4, Greenbelt, MD, USA, Goddard Earth Sciences Data and Information Services Center (GES DISC), Accessed: 11/2018, doi: 10.5067/Y67YQ1L3ZZ4R, 2015.

Hallikainen, M. and Winebrenner, D. P.: The Physical Basis for Sea Ice Remote Sensing, in: Microwave Remote Sensing of Sea Ice, Carsey, F. D. (Ed.), AGU, Washington, DC, USA, 29-46, 1992.

Haumann, F. A., Gruber, N., Münnich, M., Frenger, I., and Kern, S., Sea-ice transport driving Southern Ocean salinity and its recent trends, Nature, 537, 89-92, doi:10.1038/nature19101, 2016.

Hendricks, S., Paul, S., and Rinne, E.: ESA Sea Ice Climate Change Initiative (Sea_Ice_cci): Southern hemisphere sea ice thickness from CryoSat-2 on the satellite swath (L2P), v2.0. Centre for Environmental Data Analysis, doi:10.5285/fbfae06e787b4fefb4b03cba2fd04bc3, 2018.

Holland, P. R., Bruneau, N., Enright, C., Losch, M., Kurtz, N. T., and Kwok, R., Modeled Trends in Antarctic Sea Ice Thickness, J. Climate, 27, 3784-3801, doi:10.1175/JCLI-D-13-00301.1, 2014.

Kern, S., Ozsoy-Cicek, B., and Worby, A. P.: Antarctic Sea Ice Thickness Retrievals from ICESat: Intercomparison of Different Approaches, Remote Sens., 8, 538, doi:10.3390/rs8070538, 2016.

Kurtz, N. T. and Farrell, S. L., Large-scale surveys of snow depth on Arctic sea ice from Operation IceBridge, Geophys. Res. Lett., 38, L20505, doi:10.1029/2011GL049216, 2011.

Kurtz, N. T. and Markus, T.: Satellite observations of Antarctic sea ice thickness and volume, J. Geophys. Res., 117, C08025, doi:10.1029/2012JC008141, 2012.

Kurtz, N. T., Farrell, S. L., Studinger, M., Galin, N., Harbeck, J. P., Lindsay, R., Onana, V. D., Panzer, B., and Sonntag, J. G., Sea ice thickness, freeboard, and snow depth products from Operation IceBridge airborne data, The Cryosphere, 7, 1035-1056, doi:10.5194/tc-1035-2013, 2013.

Kurtz, N. T., Galin, N., and Studinger, M.: An improved CryoSat-2 sea ice freeboard retrieval algorithm through the use of waveform fitting, The Cryosphere, 8, 1217-1237, doi:10.5194/tc-8-1217-2014, 2014.

Kwok, R.: Simulated effects of a snow layer on retrieval of CryoSat-2 sea ice freeboard, Geophys. Res. Lett., 41, 5014-5020, doi:10.1002/2014GL060993, 2014.

Kwok, R. and Maksym, T.: Snow depth of the Weddell and Bellingshausen sea ice covers from IceBridge surveys in 2010 and 2011: An examination, J. Geophys. Res. Oceans., 119, 4141-4167, doi:10.1002/2014JC009943, 2014.

Kwok, R., Cunningham, G. F., Wensnahan, M., Rigor, I., Zwally, H. J., and Yi, D.: Thinning and Volume loss of the Arctic Ocean sea ice cover: 2003-2008, J. Geophys. Res., 114, C07005, doi:10.1029/2009JC005312, 2009.

Laxon, S., Peacock, N., and Smith, D.: High interannual variability of sea ice thickness in the Arctic region, Nature, 425, 947-950, 2003.

Laxon, S. W., Giles, K. A., Ridout, A. L., Wingham, D. J., Willatt, R., Cullen, R., Kwok, R., Schweiger, A., Zhang, J., Haas, C., Hendricks, S., Krishfield, R., Kurtz, N., Farrell, S., and Davidson, M., CryoSat-2 estimates of Arctic sea ice thickness and volume, Geophys. Res. Lett., 40, 732-737, doi:10.1002/grl.50193, 2013.

18

Legendre, L., Ackley, S. F., Dieckmann, G. S., Gulliksen, B., Horner, R., Hoshiai, T., Melnikov, I. A., Reeburgh, W. S., Spindler, M., and Sullivan, C. W.: Ecology of sea ice biota, Polar Biol., 12, 429-444, doi:10.1007/BF00243114, 1992.

Leuschen, C.: IceBridge Snow Radar L1B Geolocated Radar Echo Strength Profiles, Version 2, November 2012, Boulder, Colorado, USA, NASA National Snow and Ice Data Center Distributed Active Archive Center, doi:10.5067/FAZTWP500V70, 2014, updated 2018.

Leuschen, C., Gogineni, P., Rodriguez-Morales, F., Paden, J., and Allen, C.: IceBridge Ku-band Radar L1B Geolocated Radar Echo Strength Profiles, Version 2, October-November 2011-2012, Boulder, Colorado, USA, NASA National Snow and Ice Data Center Distributed Active Archive Center, doi:10.5067/D7DX7J7J5JN9, 2014, updated 2017.

Lewis, M. J., Tison, J. L., Weissling, B., Delille, B., Ackley, S. F., Brabant, F., and Xie, H.: Sea ice and snow cover characteristics during the winter-spring transition in the Bellingshausen Sea: An overview of SIMBA 2007, Deep-Sea Res. Pt. II, 58, 1019-1038, doi:10.1016/j.dsr2.2010.10.027, 2011.

Li, H., Xie, H., Kern, S., Wan, W., Ozsoy, B., Ackley, S., and Hong, Y.: Spatio-temporal variability of Antarctic sea-ice thickness and volume obtained from ICESat data using an innovative algorithm, Remote Sens. Environ., 219, 44-61, doi:10.1016/j.rse.2018.09.031, 2018.

Maksym, T., and Markus, T.: Antarctic sea ice thickness and snow-to-ice conversion from atmospheric reanalysis and passive microwave snow depth, J. Geophys. Res., 113, C02S12, doi:10.1029/2006JC004085, 2008.

Maksym, T., Stammerjohn, S.E., Ackley, S., and Massom, R.: Antarctic sea ice-A polar opposite?, Oceanography, 25, 140-151, doi:10.5670/oceanog.2012.88, 2012.

Markus, T. and Cavalieri, D. J.: Snow Depth Distribution over Sea Ice in the Southern Ocean from Satellite Passive Microwave Data, in: Antarctic Sea Ice: Physical Processes, Interactions and Variability, Volume 74, edited by: M. Jeffries, American Geophysical Union, 19-39, doi:10.1029/AR074p0019, 1998.

Markus, T., Massom, R., Worby, A., Lytle, V., Kurtz, N., and Maksym, T.: Freeboard, snow depth and se-ice roughness in East Antarctica from in situ and multiple satellite data, Ann. Glaciol., 52, 242-248, doi:10.3189/172756411795931570, 2011.

Markus, T., Neumann, T., Martino, A., Abdalati, W., Brunt, K., Csatho, B., Farrell, S., Fricker, H., Gardner, A., Harding, D., Jasinski, M., Kwok, R., Magruder, L., Lubin, D., Luthcke, S., Morison, J., Nelson, R., Neuenschwander, A., Palm, S., Popescu, S., Shum, C., Schutz, B., Smith, B., Yang, Y., and Zwally, H.: The Ice, Cloud, and land Elevation Satellite-2 (ICESat-2): Science requirements, concept, and implementation, Remote Sens. Environ., 190, 260–273, doi: 10.1016/j.rse.2016.12.029, 2017.

Massom, R. A., Eicken, H., Hass, C., Jeffries, M. O., Drinkwater, M. R., Sturm, M., Worby, A. P., Wu, X., Lytle, V. I., Ushio, S., Morris, K., Reid, P. A., Warren, S. G., and Allison, I.: Snow on Antarctic sea ice, Rev. Geophys., 39, 413-445, doi:10.1029/2000RG000085, 2001.

Meiners, K. M., Arndt, S., Bestley, S., Krumpen, T., Ricker, R., Milnes, M., Newbery, K., Freier, U., Jarman, S., King, R., Proud, R., Kawaguchi, S., and Meyer, B., Antarctic pack ice algal distribution: Floe-scale spatial variability and predictability from physical parameters, Geophys. Res. Lett., 44, 7382-7390, doi:10.1002/2017GL074346, 2017.

Nandan, V., Geldsetzer, T., Yackel, J., Mahmud, M., Scharien, R., Howell, S., King, J., Ricker, R., and Else, B.: Effect of Snow Salinity on CryoSat-2 Arctic First-Year Sea Ice Freeboard Measurements, Geophys. Res. Lett., 44, 10419-10426, doi:10.1002/2017GL074506, 2017.

19

Nghiem, S. V., Rigor, I. G., Clemente-Colón, P., Neumann, G., and Li, P. P., Geophysical constraints on the Antarctic sea ice cover, Remote Sens. Environ., 181, 281-292, doi:10.1016/j.rse.2016.04.005, 2016.

Onstott, R. G.: SAR Scatterometer Signatures of Sea Ice, in: Microwave Remote Sensing of Sea Ice, Carsey, F. D. (Ed.), AGU, Washington, DC, USA, 73-104, 1992.

5   Parkinson, C. L. and Cavalieri, D. J.: Antarctic sea ice variability and trends, 1979-2010, The Cryosphere, 6, 871-880, doi:10.5194/tc-6-871-2012, 2012.

Paul, S., Hendricks, S., Ricker, R., Kern, S., and Rinne, E.: Empirical parametrization of Envisat freeboard retrieval of Arctic and Antarctic sea ice based on CryoSat-2: progress in the ESA Climate Change Initiative, The Cryosphere, 12, 2437-2460, doi:10.5194/tc-12-2437-2018, 2018.

10   Price, D., Beckers, J., Ricker, R., Kurtz, N., Rack, W., Haas, C., Helm, V., Hendricks, S., Leonard, G., and Langhorne, P. J.: Evaluation of CryoSat-2 derived sea-ice freeboard over fast ice in McMurdo Sound, Antarctica, J. Glaciol., 61, 285-300, doi:10.3189/2015JoG14J157, 2015.

Perovich, D. K., Grenfell, T.C., Light, B., and Hobbs, P. V.: Seasonal evolution of the albedo of multiyear Arctic sea ice, J. Geophys. Res., 107, 20-2 – 20-13, doi:10.1029/2000JC000438, 2002.

15   Reid, P., Stammerjohn, S., Massom, R., Scambos, T., and Lieser, J., The record 2013 Southern Hemisphere sea-ice extent maximum, Ann. Glaciol., 56, 99-106, doi:10.3189/2015AoG69A892, 2015.

Ricker, R., Hendricks, S., Perovich, D. K., Helm, V., and Gerdes, R.: Impact of snow accumulation on CryoSat-2 range retrievals over Arctic sea ice: An observational approach with buoy data, Geophys. Res. Lett., 42, 4447-4455, doi:10.1002/2015GL064081, 2015.

20   Schwegmann, S., Rinne, E., Ricker, R., Hendricks, S., and Helm, V.: About the consistency between Envisat and CryoSat-2 radar freeboard retrieval over Antarctic sea ice, The Cryosphere, 10, 1415-1425, doi:10.5194/tc-10-1415-2016, 2016.

Stiles, W. H. and Ulaby, F.T.: Dielectric Properties of Snow, RSL Tech. Rep. 527-1, Accession Number ADP000148, 91–103, 1980.

Studinger, M.: IceBridge ATM L2 Icessn Elevation, Slope, and Roughness, Version 2, October-November 2011-2012, Boulder, Colorado, USA, NASA National Snow and Ice Data Center Distributed Active Archive Center, doi:10.5067/CPRXXK3F39RV, 2014, updated 2018.

25   Tiuri, M., A. Sihvola, E. Nyfors, and M. Hallikainen, The complex dielectric constant of snow at microwave frequencies, IEEE J. Ocean. Eng., 9, 377–382, 1984.

Turner, J., and Comiso, J., Solve Antarctica's sea-ice puzzle, Nature, 547, 275-277, doi:10.1038/547275a, 2017.

Turner, J., Phillips, T., Marshall, G. J., Hosking, J. S., Pope, J. O., Bracegirdle, T. J., and Deb, P., Unprecedented springtime retreat of Antarctic sea ice in 2016, Geophys. Res. Lett., 44, 6868-6875, doi:10.1002/2017GL073656, 2017.

30   Ulaby, F. T., Moore, R. K., and Fung, A. K.: Microwave Remote Sensing, vol. 2, Radar Remote Sensing and Surface Scattering and Emission Theory, Artech House, Norwood, Mass., 848–851, 943–944, 1986.

Webster, M., Gerland, S., Holland, M., Hunke, E., Kwok, R., Lecomte, O., Massom, R., Perovich, D., and Sturm, M.: Snow in the changing sea-ice systems, Nat. Clim. Change, 8, 946-953, doi: 10.1038/s41558-018-0286-7, 2018.

Willatt, R., Giles, K. A., Laxon, S. W., Stone-Drake, L., and Worby, A. P.: Field Investigations of Ku-Band Radar Penetration Into Snow Cover on Antarctic Sea Ice, IEEE T. Geosci. Remote., 48, 365-372, doi:10.1109/TGRS.2009.2028237, 2010.

Willatt, R., Laxon, S., Giles, K., Cullen, R., Haas, C., and Helm, V.: Ku-band radar penetration into snow cover on Arctic sea ice using airborne data, Ann. Glaciol., 52, 197–205, 2011.

Wingham, D. J., Francis, R. C., Baker, S., Bouzinac, C., Cullen, R., de-Chateau-Thierry, P., Laxon, S. W., Mallow, U., Mavrocordatos, C., Phalippou, L., Ratier, G., Rey, L., Rostan, F., Viau, P., and Wallis, D.: CryoSat: A mission to determine the fluctuations in the Earths land and marine ice fields, Adv. Space Res., 37, 841–871, doi:10.1016/j.asr.2005.07.027, 2006.

Weissling, B. P., and Ackley, S.F.: Antarctic sea-ice altimetry: scale and resolution effects on derived ice thickness distribution, Ann. Glaciol., 52, 225–232, doi:10.3189/172756411795931679, 2011.

Worby, A. P., Massom, R. A., Allison, I., Lytle, V. I., and Heil, P.: East Antarctic Sea Ice: A Review of Its Structure, Properties and Drift, In: Antarctic Sea Ice: Physical Processes, Interactions and Variability, Antarctic Research Series, AGU, 74, 89-122, doi: 10.1029.AR074p0041, 1998.

Worby, A. P., Geiger, C. A., Paget, M. J., Van Woert, M. L., Ackley, S. F., and DeLiberty, T. L.: Thickness distribution of Antarctic sea ice, J. Geophys. Res.-Oceans, 113, C05S92, doi:10.1029/2007JC004254, 2008.

Xie, H., Ackley, S. F., Yi, D., Zwally, H. J., Wagner, P., Weissling, B., Lewis, M., and Ye, K.: Sea-ice thickness distribution of the Bellingshausen Sea from surface measurements and ICESat altimetry, Deep-Sea Res. Pt. II, 58, 1039-1051, doi:10.1016/j.dsr2.2010.10.038, 2011.

Yi, D., Kurtz, N., Harbeck, J., Kwok, R., Hendricks, S., and Ricker, R.: Comparing Coincident Elevation and Freeboard from IceBridge and Five Different CryoSat-2 Retrackers, IEEE Trans. Geosci. Remote Sens., 1-11, doi: 10.1109/TGRS.2018.2865257, 2018.

Zatko, M. C. and Warren, S. G.: East Antarctic sea ice in spring: spectral albedo of snow, nilas, frost flowers and slush, and light-absorbing impurities in snow, Ann. Glaciol., 56, 53-64, doi:10.3189/2015AoG69A574, 2015.

Zwally, H. J., Yi, D., Kwok, R., and Zhao, Y.: ICESat measurements of sea ice freeboard and estimates of sea ice thickness in the Weddell Sea, J. Geophys. Res. -Oceans, 113, C02S15 ,doi: 10.1029/2007JC004284, 2008.
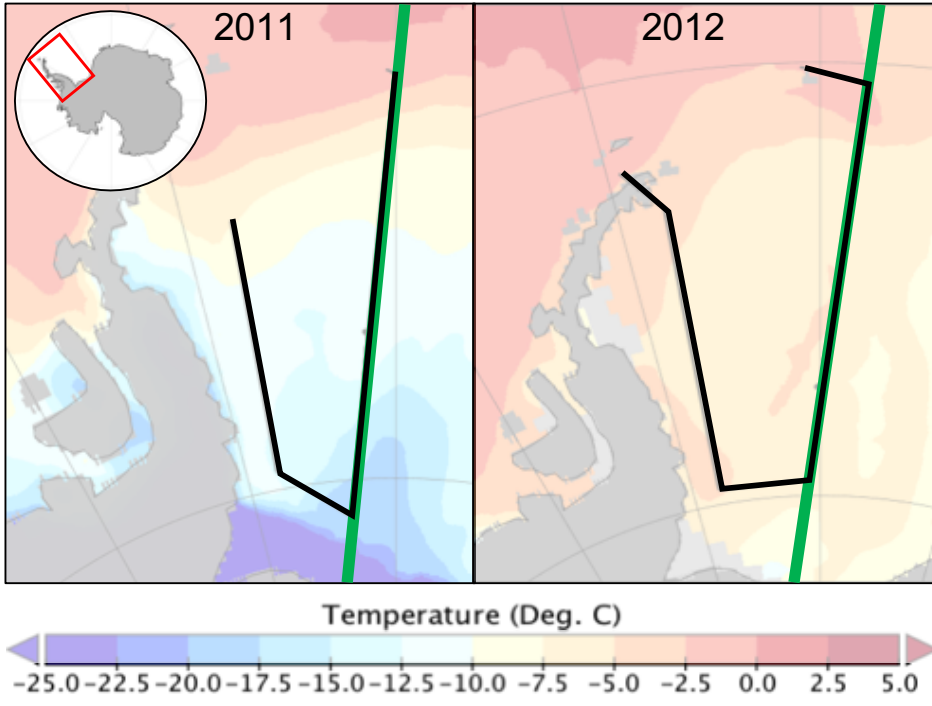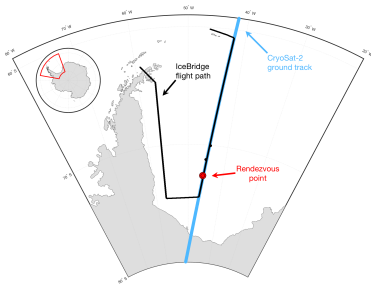
Figure 1: Maps of the Operation IceBridge 13 October 2011 (left) and 07 November 2012 (right) Sea Ice Endurance campaign flight paths (in black) along with the contemporaneous CryoSat-2 ground track (in green) and rendezvous point. Flight paths are overlaid on hourly average sea ice surface temperatures from MERRA-2 at the midpoint time of the IceBridge flight (MERRA-2 data from: doi: 10.5067/Y67YQ1L3ZZ4R). The 13 October 2011 campaign follows a similar path.
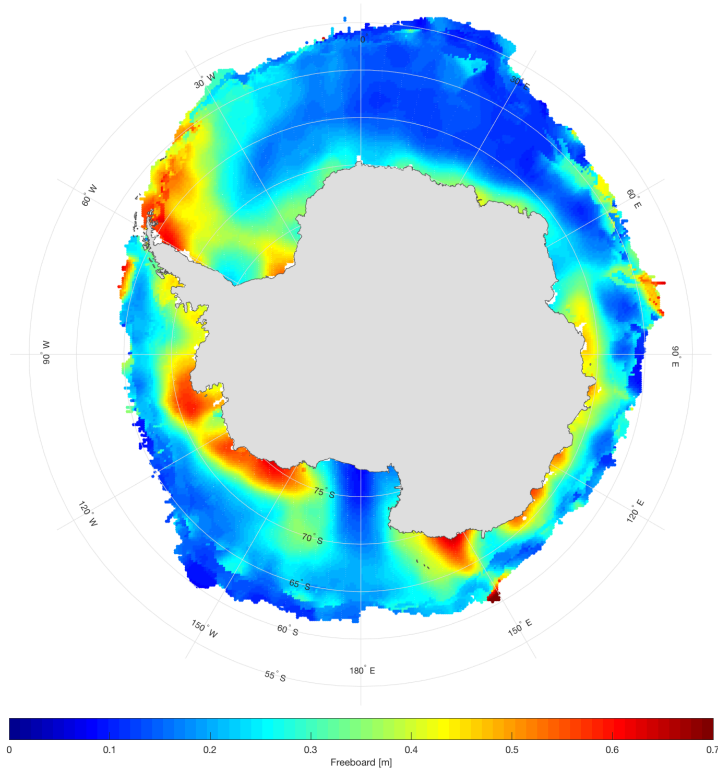
Figure 2: ICESat austral spring mean freeboard, consisting of measurements taken in October and November 2003-2007.
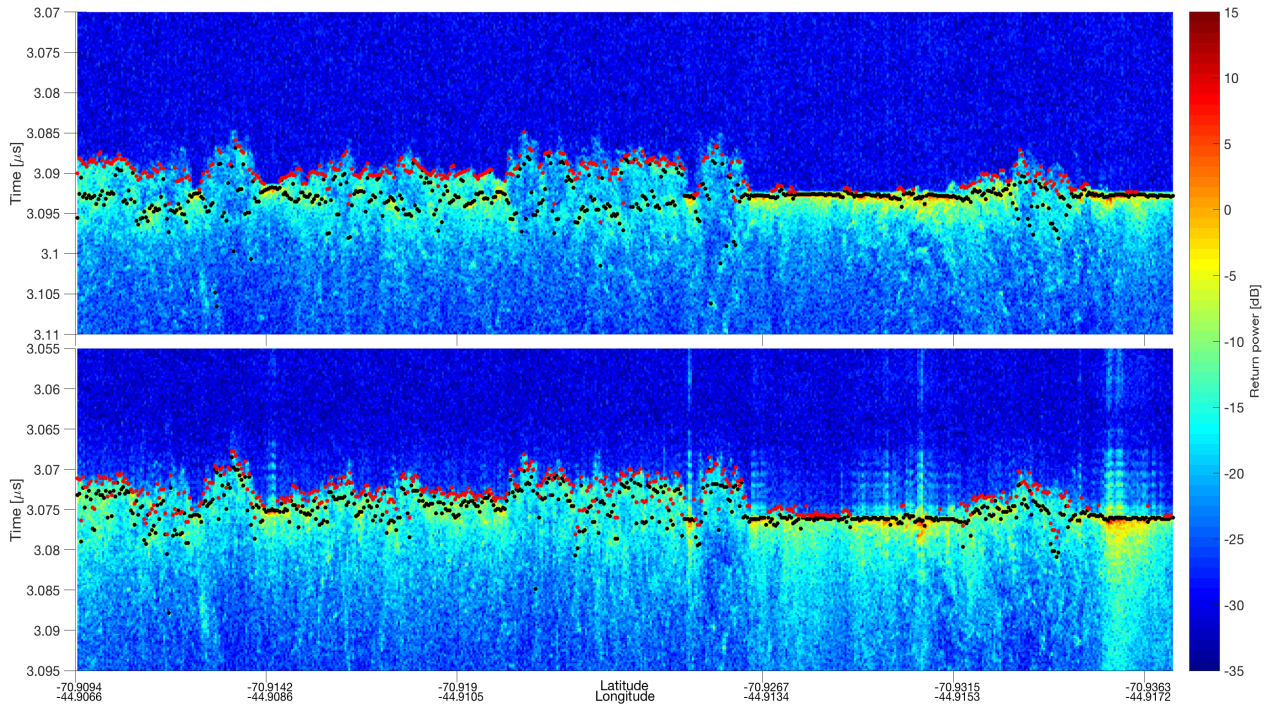
5   **Figure 3:** Example echograms from Operation IceBridge snow radar (top) and Ku-band radar (bottom) taken from the November 2012 Sea Ice Endurance campaign. Black points denote locations of maximum power and red points denote the first location where the power rises 10dB above the noise level, both found from the peak-picking algorithm discussed in text. The length of the transect covered in this echogram is 3.02km. The mean (standard deviation) noise level for the snow radar is found to be -29.1 dB (1.39 dB) while the signal level at the air-snow interface is found to

23

be -16.8 dB (1.47 dB). For the Ku-band altimeter, the noise level is found to be -30.3 dB (1.32 dB) while the air-snow interface signal level is found to be -17.9 db (2.09 dB), showing the surface return is well above the noise for both instruments.
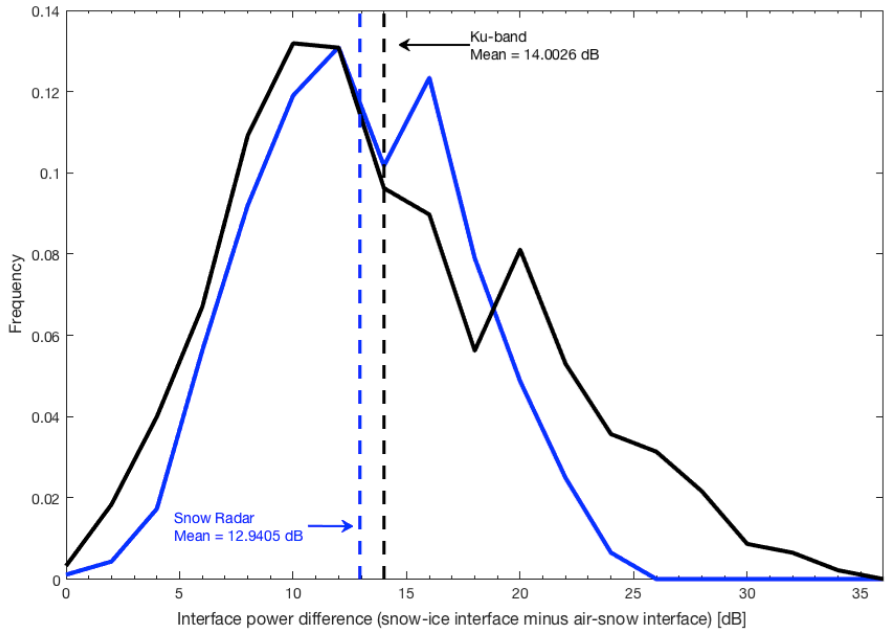
Figure 4: Frequency distributions of the difference in air-snow interface power from snow-ice interface power taken from the November 2012 IceBridge Sea Ice Endurance campaign. The blue curve represents the snow radar, while the black curve represents the Ku-band radar. Note that the locations of the air-snow and snow-ice interfaces are approximations found from the peak-picking algorithm (Fig. 3) and are not exactly the expected backscatter coefficients from the two layers.
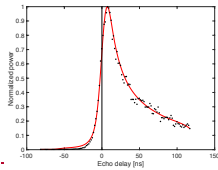
~~**Figure 5:** An example sea ice floe waveform and fit from October 2016. Black points are CryoSat-2 level 1 B data and the red curve is the modeled fit waveform using this algorithm. This particular waveform has a resnorm of 0.065, representing a good fit.~~
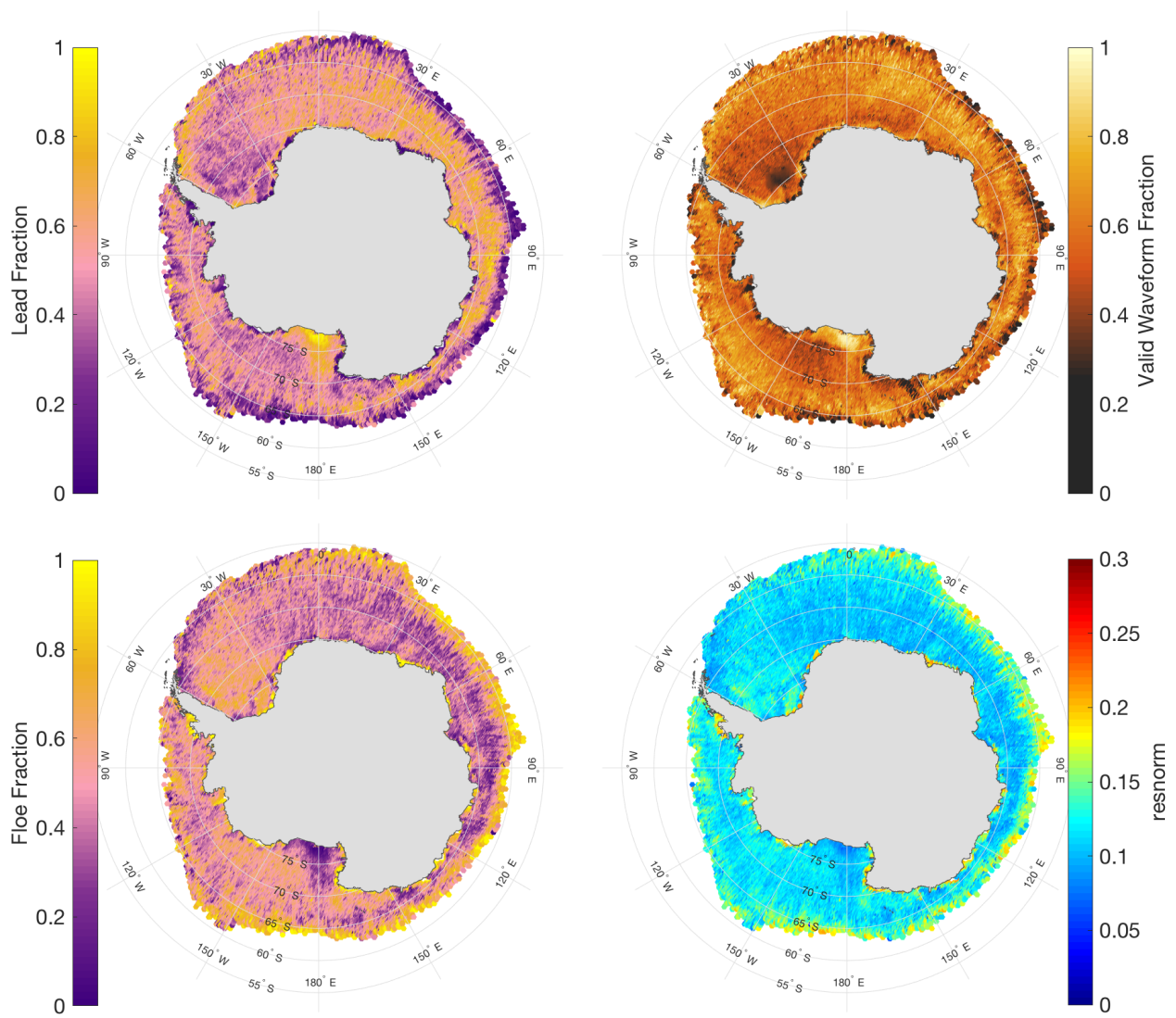
Figure 5: October 2011-2017 average maps of lead-type waveform fraction (top-left), floe-type waveform fraction (bottom-left), valid waveform fraction (top-right), and resnorm value (bottom-right).
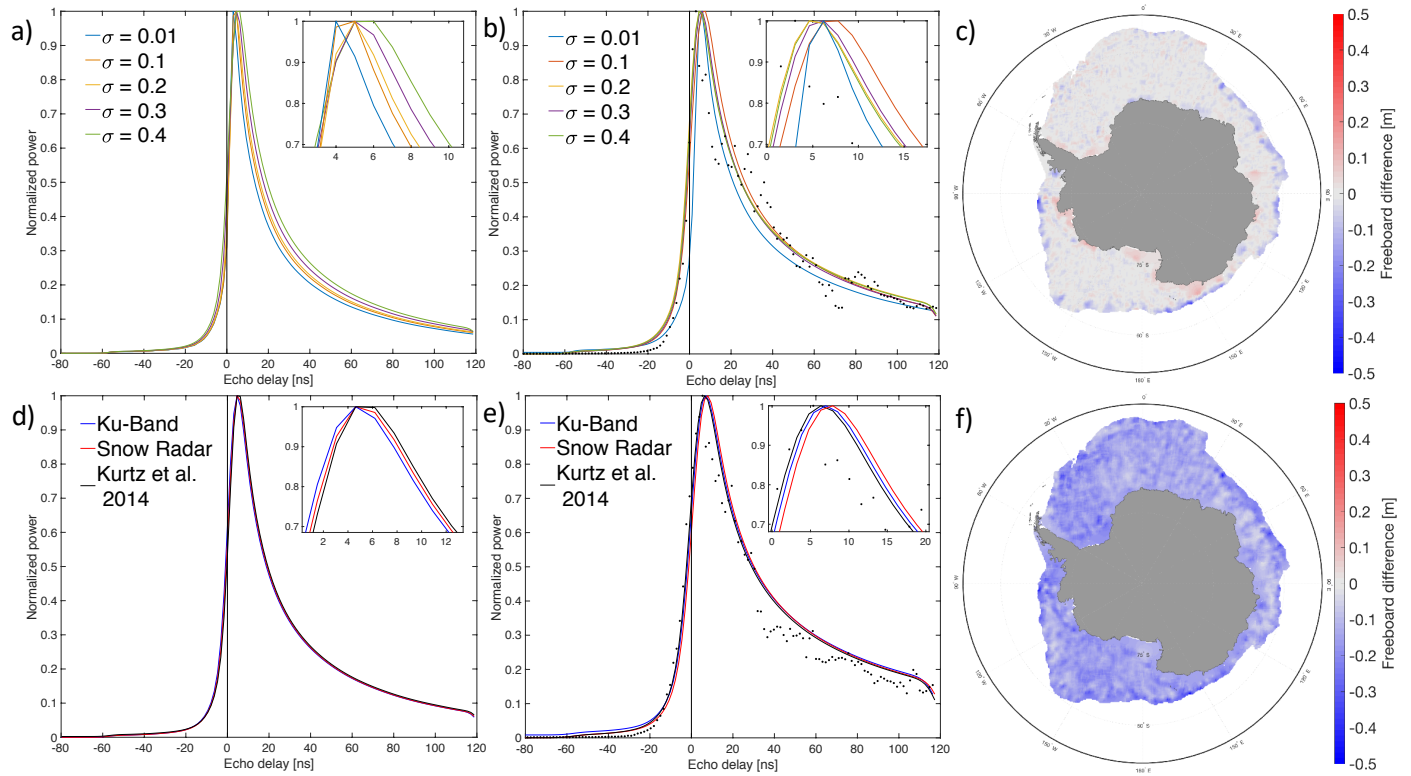
Figure 6: A sensitivity study of two initial guess parameters: the standard deviation of surface height, σ, and the total backscatter, σ^0. (a) modeled waveform (before fitting) varying the initial guess value of σ between 0.01 (very smooth surface) and 0.4 (rough surface). (b) waveforms fit to CryoSat-2 data varying the initial guess value of σ between 0.01 and 0.4. (c) October 2016 average freeboard difference: σ = 0.35 as the initial guess – σ = 0.15 as the initial guess. (d) as in (a) using three different backscatter parameterizations taken from the OIB Ku-Band radar profile, Snow Radar profile, and Kurtz et al. 2014. (e) as in (b) with the three different backscatter parameterizations. (f) as in (c) showing Kurtz et al. 2014 backscatter as the initial guess – Ku-Band backscatter as the initial guess. Inlaid plots are zoomed in on the waveform peaks. The methodology for freeboard calculations is explained in later sections of the paper.

26
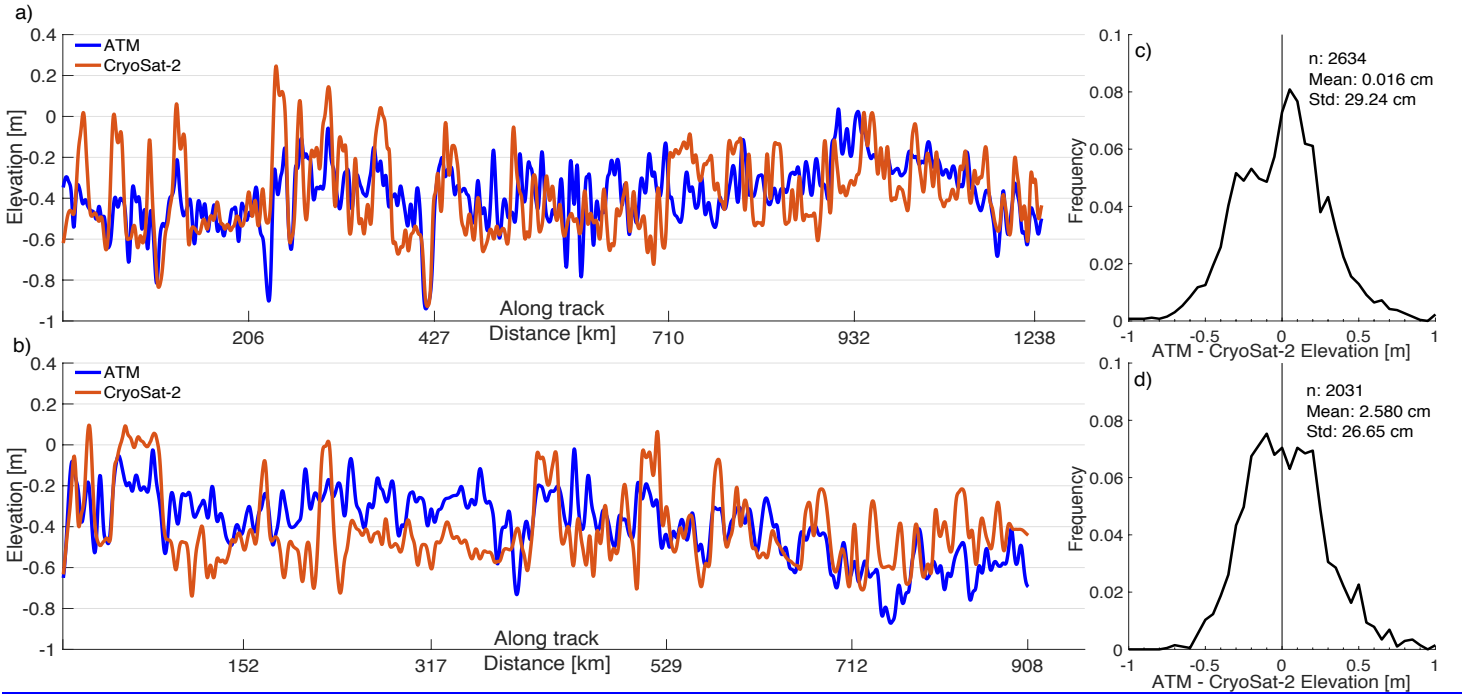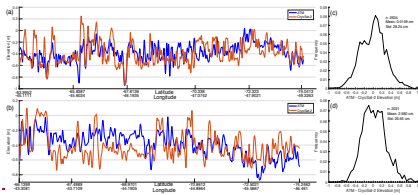
Figure 6Figure 7: Surface (air-snow interface) elevation profiles of Operation IceBridge ATM (blue) and CryoSat-2 (orange) from the October 2011 (a) and November 2012 (b) campaigns. Frequency distributions of the elevation difference (ATM – CryoSat-2) along the 2011 (c) and 2012 (d) profiles are also shown. The mode of the differences is 0.025m in 2011 and -0.24m in 2012. The 2011 profile contains measurements from -63.99° N, -45.11° W to -75.04° N, -49.33° W while the 2012 profile contains measurements from -66.14° N, -43.31° W to -74.25° N, -46.46° W.
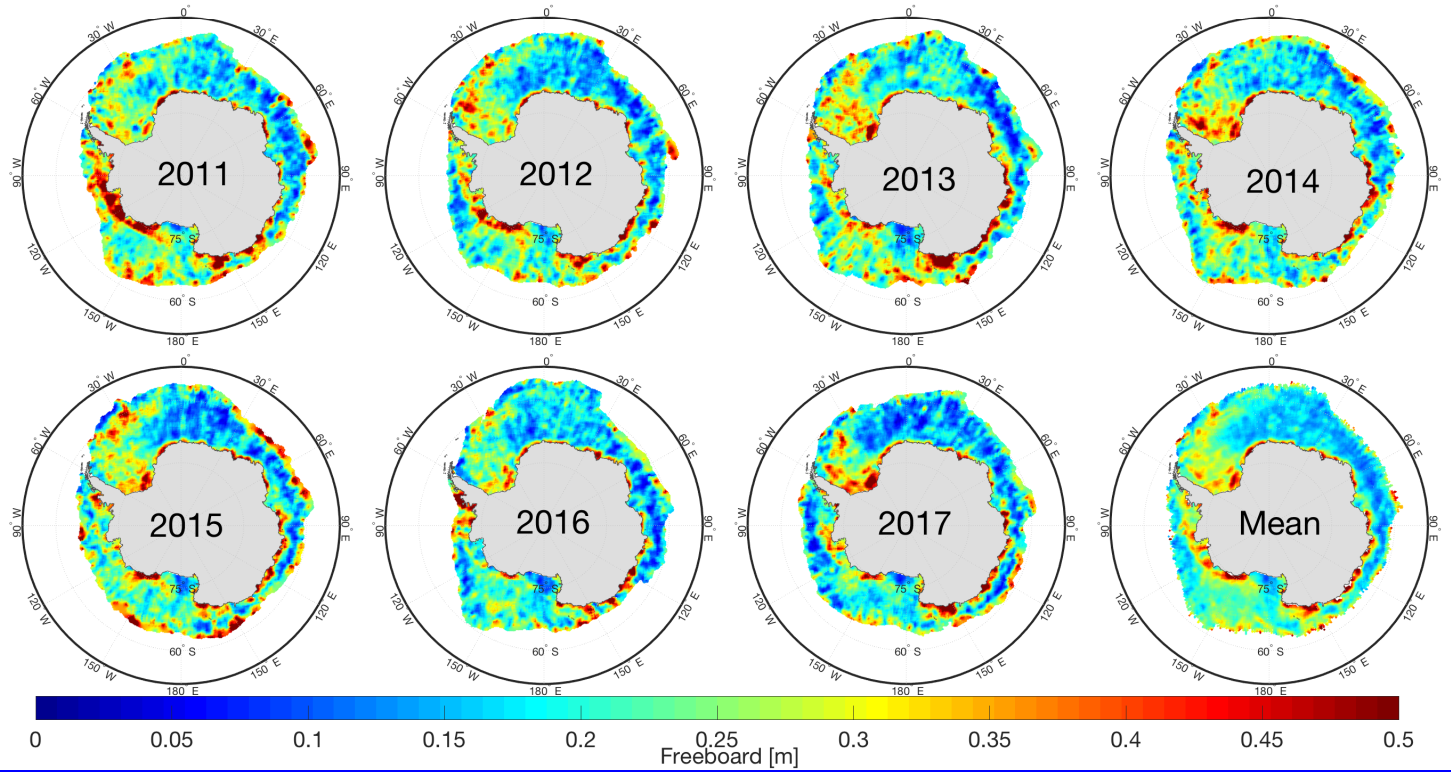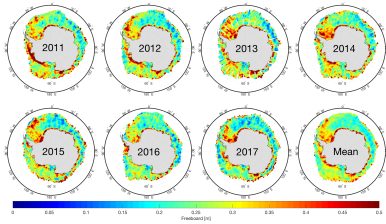
Figure 7Figure 8: October monthly average snow freeboard from 2011-2017, as well as the mean of all years, found using this retrieval method. Note that data gaps in 2013 are a result of missing CryoSat-2 level 1B data from 02 October – 11 October 2013.
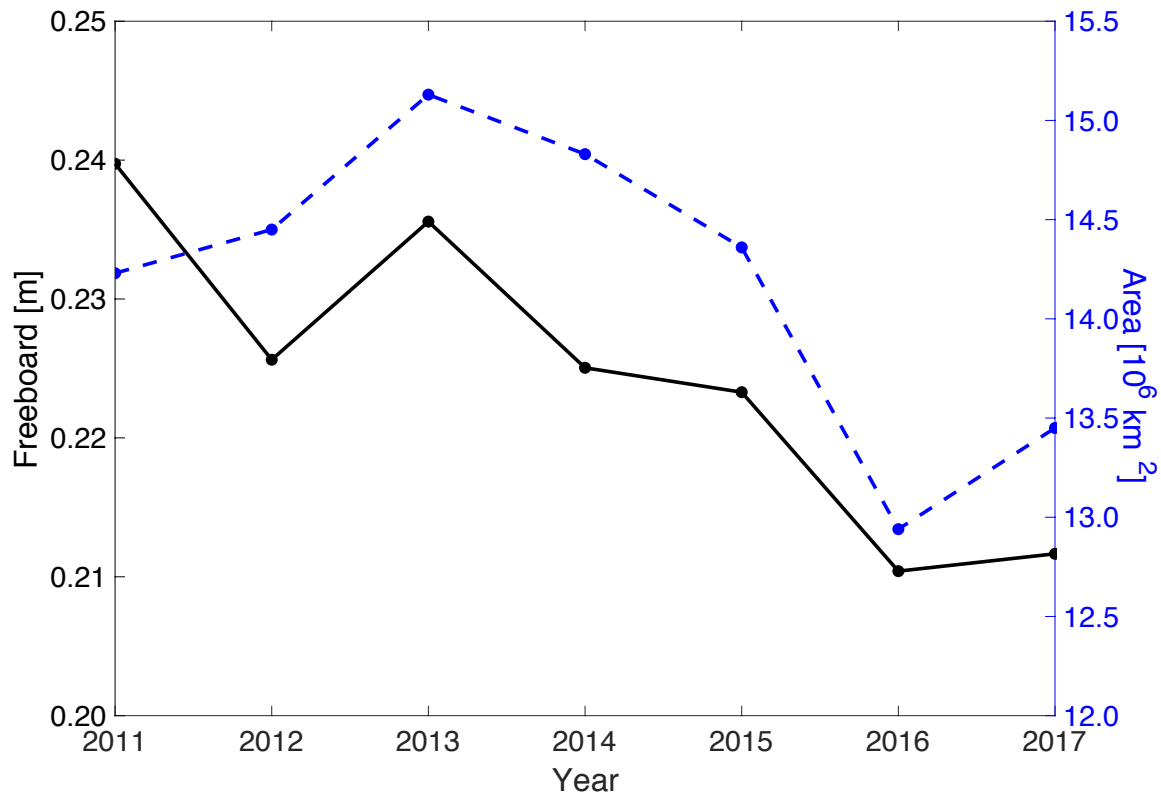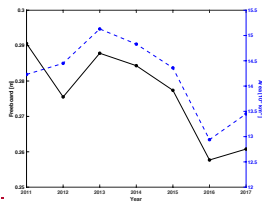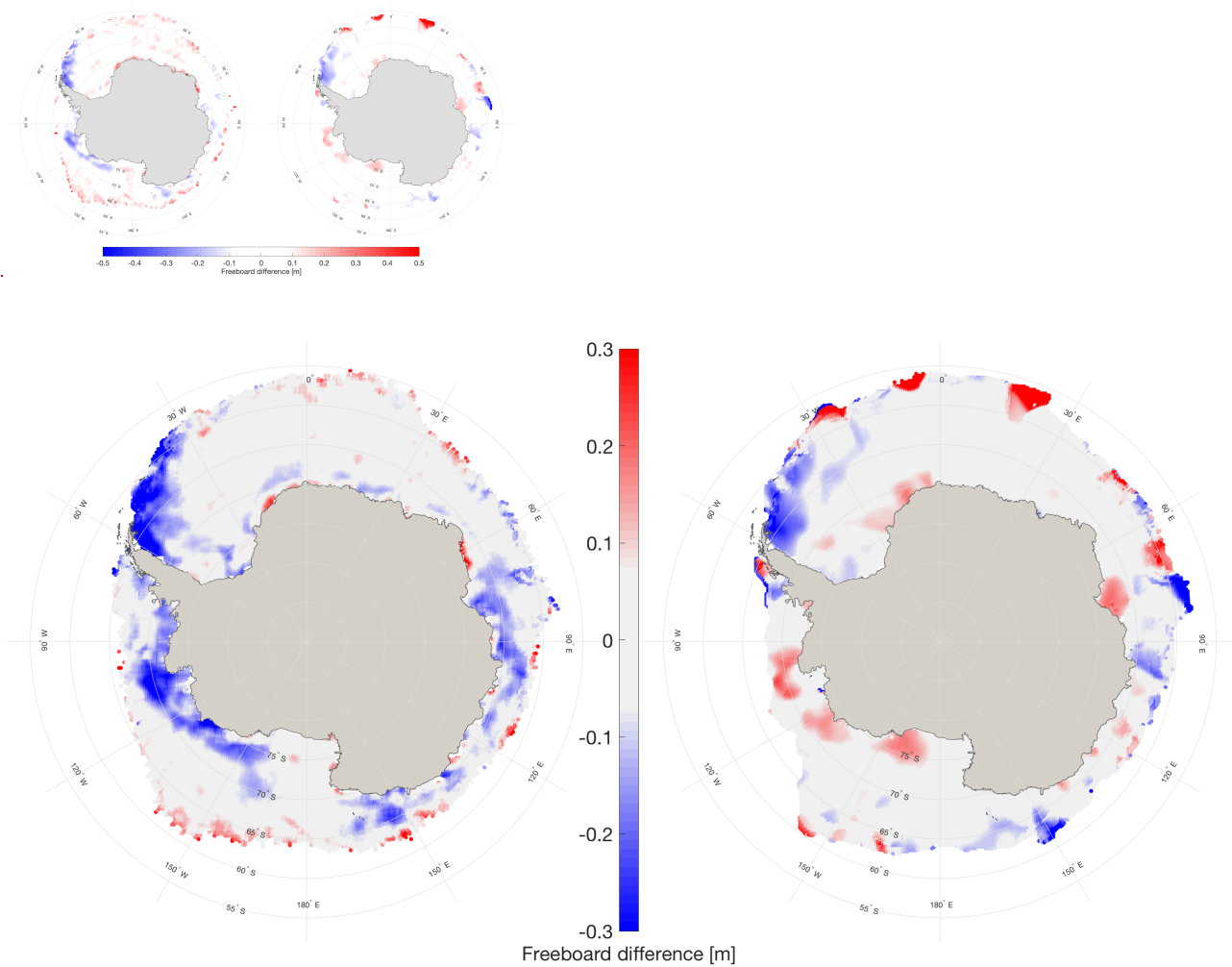
5

28

Figure 8Figure 9: October monthly average Antarctic snow freeboard (black) and total sea ice area (blue) for reference. Sea ice area data are gathered from NSIDC (Fetterer et al., 2017) and can be found at nsidc.org/data/G02135.

Figure 9Figure 10: Snow freeboard differences showing (left) CryoSat-2 October 2011-2017 average minus ICESat spring 2003-2007 average and (right) ICESat spring 2006 average minus ICESat spring 2003-2007 average. 2006 is included as an example year to highlight the interannual variability in the freeboard distribution.
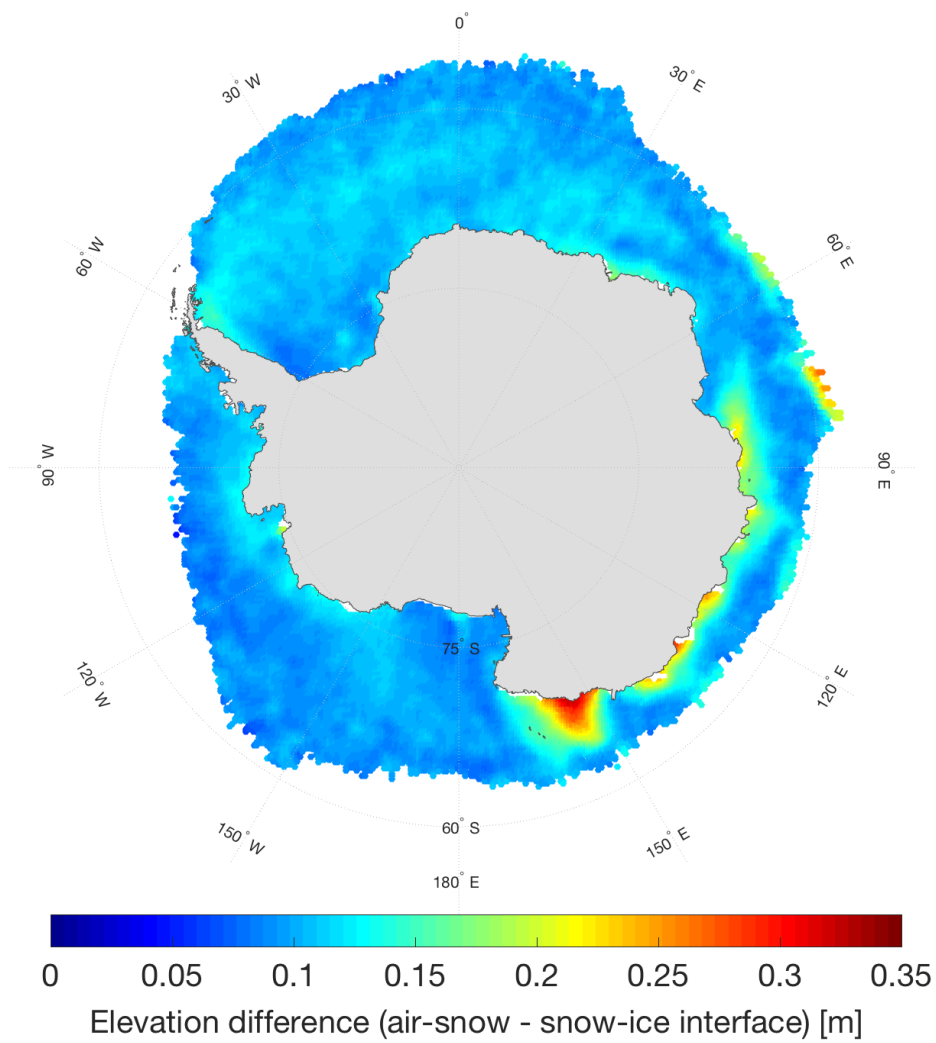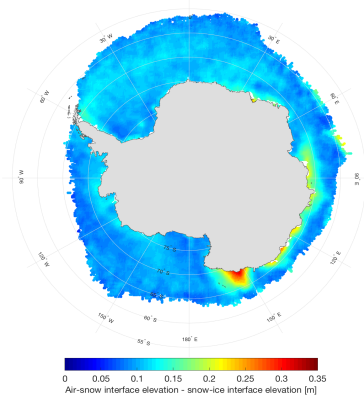
Elevation difference (air-snow - snow-ice interface) [m]

Figure 10Figure 11: October 2011-2017 average difference between the retrieved air-snow and snow-ice interfaces as an exploration into the potential retrieval of snow depth.